# Differential Amplification of Gene Expression in Lens Cell Lines Conditioned to Survive Peroxide Stress

*Abraham Spector,*[1] *Dayu Li,*[1,2] *Wanchao Ma,*[1,2] *Fang Sun,*[1] *and Paul Pavlidis*[3]

**Purpose.** The response of lens systems to oxidative stress is confusing. Antioxidative defense systems are not mobilized as expected, and unanticipated defenses appear important. Therefore, mouse lens cell lines conditioned to survive different peroxide stresses have been analyzed to determine their global changes in gene expression.

**Methods.** The immortal mouse lens epithelial cell line αTN4-1 was conditioned to survive 125 μM $H_2O_2$ (H cells) or a combination of both 100 μM tertiary butyl hydroperoxide (TBHP) and 125 μM $H_2O_2$ (HT cells), by a methodology previously described. The total RNA was isolated from the different cell lines and analyzed with oligonucleotide mouse expression microarrays. Four microarrays were used for each cell line. Microarray results were confirmed by real-time RT-PCR.

**Results.** A new cell line resistant to both 125 μM $H_2O_2$ and 100 μM TBHP was developed, because cells resistant to $H_2O_2$ were killed by TBHP. Analysis of classic antioxidative enzyme activities showed little change between cells that survive $H_2O_2$ (H) and those that survive $H_2O_2$ and TBHP (HT). Therefore, the global change in gene expression in these cell lines was determined with gene expression microarrays. The fluorescent signal changes of the genes within the three cell lines, H, HT, and control (C), were analyzed by statistical methods including Tukey analysis. It was found that from the 12,422 gene fragments and expressed sequence tags (ESTs) analyzed—based on a one-way ANOVA with a stringent cutoff of one false positive per 1000 genes and correcting for microarray background and noise—approximately 950 (7.6%) genes had a significant change in expression in comparing the C, H, and HT groups. A small group of antioxidative defense genes were found in this population, including catalase, members of the glutathione (GSH)-*S*-transferase family, NAD(P)H menadione oxidoreductase 1, and the ferritin light chain. The remaining genes are involved in a broad spectrum of other biological systems. In the HT versus H comparison, only a few genes were found that had increased expression in the HT line compared with expression in the H line, including GSH-*S*-transferase alpha 3 and hephaestin. Many genes that are frequently considered antioxidative defense genes, including most of the GSH peroxidases, unexpectedly showed little change.

**Conclusions.** An unusual and generally unexpected small group of antioxidative defense genes appear to have increased expression in response to $H_2O_2$ stress. Cell lines resistant to $H_2O_2$ do not appear to survive challenge with another type of peroxide, TBHP, a lipid peroxide prototype. However, acquisition of TBHP resistance by H cells was found to be accompanied by significantly amplified expression of only a few additional antioxidative defense genes. Many of the amplified genes do not appear to be involved with antioxidative systems, reflecting the complexity of the cells' response to oxidative stress. (*Invest Ophthalmol Vis Sci.* 2002;43:3251–3264)

There is a large literature relating oxidative stress to a variety of diseases,[1,2] such as cardiovascular,[3,4] intestinal,[5] pulmonary,[6] mitochondrial,[7] and neurodegenerative disease,[8] including Alzheimer's disease [9] and Parkinson's disease.[10] Thus, it is not surprising that, when the eye is subjected to oxidative stress, cataract develops in the lens, which is in a low-oxygen environment and has only a single layer of actively metabolizing epithelial cells.[11–18]

It has been shown that $H_2O_2$ is elevated in the aqueous, vitreous, and lenses in eyes of patients with maturity-onset cataract,[19–21] and this increase correlates with extensive oxidation of lens components.[11,22–24] Furthermore, $H_2O_2$ can cause opacification of the lens in organ culture at concentrations found in patients with cataract.[17,25]

To investigate the response to peroxide stress is complex. The lens contains only a single layer of epithelial cells, where most of the metabolic activity resides and a few layers of newly formed fiber cells that still have the biological machinery to make new protein directed by DNA. It is this thin layer of cells that is primarily responsible for the organ's defense against oxidative stress. Even this situation is complex, however, in that the cells in the vicinity of the visual axis do not divide; but moving toward the equator, there is a zone in which cell division occurs, and finally, in the bow region, terminal differentiation is initiated, generating the formation of the fiber cells and the gradual disintegration of the protein synthesizing apparatus. Each cell type would be expected to respond in a unique manner to oxidative stress. Furthermore, the cellular response is not simple, involving shutting down some metabolic systems, increasing energy production, stimulating DNA repair systems, activating programmed apoptosis in some cells and stimulating the mobilization of antioxidative defenses. To sort out from this complex and time-dependent variation of gene expression and other mechanisms for modifying cell biology, those genes that specifically are capable of protecting the cell so that it can survive the stress is difficult at best.

Another approach is to investigate a homogeneous immortal cell type, such as the immortal murine lens epithelial cell line αTN4-1. Unlike primary lens cell cultures, there are relatively few changes from one generation to another. Gene expression is relatively constant. Therefore, this cell line has been conditioned to survive peroxide stress.

However, the relationship to the lens of the simian virus (SV)40–transformed cells and their conditioned progeny should be considered. Even though the conditioned cells retain morphologic and cell growth features similar to those of un-

From the [1]Department of Ophthalmology and the [3]Columbia Genome Center, Columbia University, New York, New York.

[2]Contributed equally to this work.

Supported by grants from the National Eye Institute, Research to Prevent Blindness, Research to Cure Cataract Foundation, and the Department of Ophthalmology, Columbia University.

Submitted for publication August 27, 2001; revised April 30, 2002; accepted June 5, 2002.

Commercial relationships policy: N.

The publication costs of this article were defrayed in part by page charge payment. This article must therefore be marked "*advertisement*" in accordance with 18 U.S.C. §1734 solely to indicate this fact.

Corresponding author: Abraham Spector, Department of Ophthalmology, Columbia University, 630 West 168th Street, New York, NY 10032; as42@columbia.edu.

conditioned cells and their appearance is not significantly different from lens cell cultures, their cell biology is clearly different.[26] This is also true of primary lens cell cultures, which lose many of their lens characteristics with passage. In this investigation, genes were found that were not expressed in unconditioned cell lines but were activated in the conditioned cell preparations. It would be expected that conditioned cells would have modified gene expression precisely to survive their new environment. The immortal cells also have been modified to take on characteristics required for eternal life. Thus, can information obtained from such modified cells be applied to the lens systems? The definitive answer cannot be forthcoming until the antioxidative defenses of the conditioned cell lines have been defined and the lens, enriched with such defenses, challenged with oxidative stress. If the lens remains transparent, then the exercise has been successful. However, it should be noted that work with other immortal cell systems such as MDCK,[27,28] COS,[29,30] CHO,[31,32] HeLa,[33,34] and 3T3[35,36] are widely used based on the assumption that biological systems are basically similar and that observations made in widely divergent cell types are applicable to each other. Furthermore, in these systems, this assumption has been confirmed repeatedly.

Analysis of the $H_2O_2$-conditioned cells indicated that not only were $H_2O_2$ detoxification systems amplified but repair systems appeared more effective.[26] The unexpected finding that some GSH-*S*-transferases were markedly increased in activity and that catalase and not GSH peroxidase appeared to be the major $H_2O_2$-degrading enzyme indicated that our understanding of how the cell defends itself against $H_2O_2$ stress is incomplete. Therefore, to find the key genes involved with antioxidative defense, a global approach is required. The biology of the cell is controlled by gene expression. Thus, a reasonable rationale to assess modification in cell biology resulting from $H_2O_2$ conditioning is to determine changes in gene expression. Modification of gene expression in response to $H_2O_2$ stress has previously been shown for selective genes,[37–39] but the entire genome has not been analyzed.

In the present work, murine expression high-density microarrays (Affymetrix, Santa Clara, CA), containing probe sets for approximately 12,400 gene fragments and expressed sequence tags (ESTs), were used to determine differential modification of gene expression in $H_2O_2$-conditioned cells (H line) and cells conditioned with both $H_2O_2$ and a lipid peroxide prototype, tertiary butyl hydroperoxide (TBHP), the HT line. We first determined that the array analysis is reliable. Then, using a rigorous statistical level of stringency (one false-positive selection in 1000 genes), we compared mRNA from four independent preparations of control cells (C cells) with four independent preparations from both the H and HT lines. An unusual group of antioxidative genes were found to have significant changes in expression. A few other interesting antioxidative defense genes with higher probabilities of error were also examined.

## Materials and Methods

### Cell Conditioning

αTN4-1, an immortal murine lens epithelial cell line, generously provided by Paul Russell, National Eye Institute (Bethesda, MD), was used in all work. The $H_2O_2$-conditioned cells (H) were prepared as previously described.[26] The cells conditioned to withstand both an $H_2O_2$ and a TBHP stress (HT cells) were prepared in a similar manner. Briefly, approximately 200,000 cells were subcultured in a 35-mm dish in 2 mL minimum essential medium (MEM, cat. no. 41500-034; Gibco BRL, Grand Island, NY), supplemented with $NaHCO_3$, 2.2 g/L medium (pH 7.2); 100 U penicillin and 100 μg streptomycin/mL medium (cat. no. 1540-122; Gibco BRL); Fungizone, 2.5 mg/L medium (cat. no. 15295-017); and fetal bovine serum (cat. no. SH30070.02; Hyclone, Logan, UT) to give a final concentration of 10%. This is the standard medium. After overnight incubation at 37°C in 5% $CO_2$, the medium was replaced with 4 mL standard medium containing 125 μM $H_2O_2$ and various concentrations of TBHP. Every 24 hours, additional aliquots of $H_2O_2$ and TBHP were added to give the desired concentration. Culture medium was changed every 3 days. Cells were subcultured when they were approximately 80% confluent and after approximately 16 hours were again exposed to the peroxides. During a period of a few months, the TBHP concentration was gradually increased from a starting concentration of 25 μM to a final concentration of 100 μM, whereas the $H_2O_2$ concentration was maintained at 125 μM. H cells and C cells were maintained in an identical manner with 125 μM $H_2O_2$ or in standard medium, respectively. Cell viability was determined by cell counting and trypan blue staining, as previously described.[26]

### Enzyme Assays

All enzyme assays were conducted by methodologies previously described.[26]

### Isolation of Total RNA

Total RNA was isolated from $1 \times 10^7$ cells removed from 80% confluent cultures using an RNA isolation kit (cat. no. 74104; RNeasy Mini Kit, Qiagen, Valencia, CA).

### Preparation of cRNA

Approximately 30 μg total RNA was used to prepare double-stranded cDNA using a commercial system (SuperScript Choice; Gibco BRL) and a T7-$(dT)_{24}$ primer: 5′-GGCCAGTGAATTGTAATACGACTCACTATA-GGGAGGCGG-$(dT)_{24}$-3′ for first-strand cDNA synthesis. After synthesis of the second-strand cDNA, the double-stranded cDNA was then purified with Phase Lock Gels (Brinkmann Instruments, Inc., Boulder, CO), phenol-chloroform extraction and ethanol precipitation. An RNA transcript labeling kit (product code 42655; Enzo Diagnostic, Inc., Farmingdale, NY) was then used to prepare a biotin-labeled cRNA. The cRNA was purified using a spin column (RNeasy; Qiagen) followed by ethanol precipitation. The cRNA was quantified and examined by gel electrophoresis. The cRNA was then fragmented at 94°C for 35 minutes.

### Gene Microarray Analysis

The use of oligonucleotide expression microarrays (Affymetrix) is now a frequently used methodology for determining gene expression. The methodology has been described in numerous publications.[40–42] Briefly, the fragmented biotin-labeled cRNA was hybridized to a mouse expression microarray (MG-U74A Ver. 2; Affymetrix), at the Genome Center of the College of Physicians and Surgeons, Columbia University, and stained with streptavidin phycoerythrin. The hybridized components were detected by fluorescence laser scanning and confocal localization and then analyzed on computer (Microarray Suite, ver. 5.0, Affymetrix; and Excel; Microsoft, Redmond, WA). Each microarray contained two groups of approximately 16 twenty-five–residue oligonucleotides for each of the 12,422 probe sets and ESTs as well as internal standards. Each member of one group was a perfect complimentary match for a particular segment of a given gene fragment or EST. The second group contained a single base mismatch in the middle of each of the oligos. Thus, one probe set contains approximately 32 oligonucleotides for each gene fragment or EST, giving a total of over 400,000 oligonucleotides plus standards on the microarray. The oligonucleotides for each gene fragment are distributed on the microarray and collated by computer for further analysis.

It should be noted that in some cases, there is more than one probe set for the same gene. The probe sets recognize different sections of the gene, including up and down stream and splicing regions. In such cases, there may be considerable differences in hybridization and, thus, the recognized expression of the gene. In most cases, only probe sets

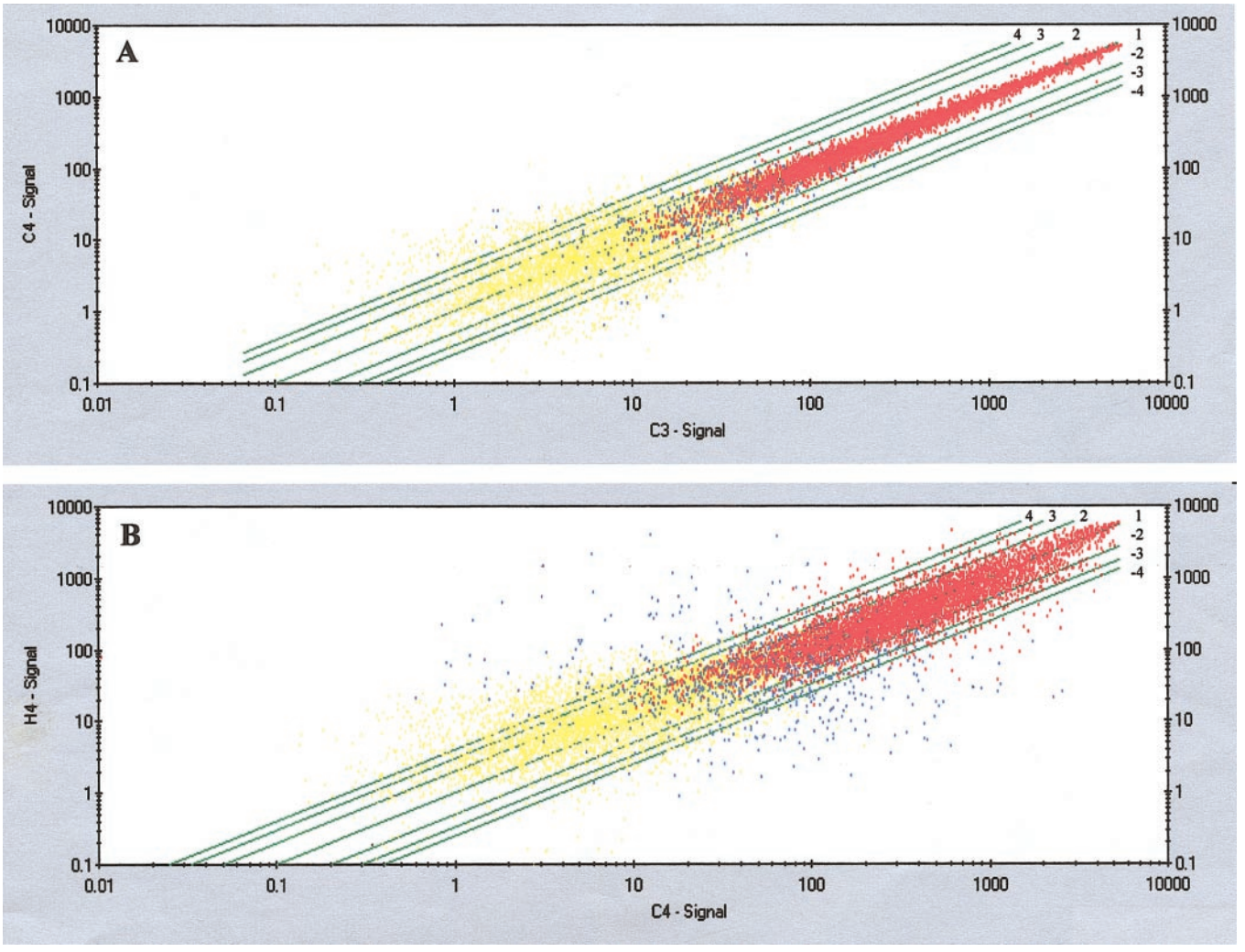


**Figure 1.** Typical scatterplots of the microarray signal intensity of 12,422 genes and ESTs. (**A**) Comparison of two arrays prepared from the C line. (**B**) Comparison of two arrays, one prepared from the H line and the other from the C line. If there is no change in expression, a ratio of 1 would be found. This is indicated on the graph by the line labeled 1. The outer lines indicate a ± fourfold change in signal intensity. Lines showing a ± three- and a ± twofold change are also presented. *Red points*: gene expression present in both arrays; *blue points*: marginal or absent calls based on software analysis in one array; *yellow points*: signals that are marginal or have an absent call in both arrays.

showing the strongest fluorescent signal intensities were used. The actual fluorescent signal levels and present, absent, and marginal calls determined by the software program for each of the 12,422 probe sets in each of four control (C), four $H_2O_2$-conditioned (H) and four $H_2O_2$+TBHP–conditioned (HT) microarrays are shown in electronic folder 1, available at http://www.iovs.org/cgi/content/full/43/10/3251/DC1. ANOVA values reflecting the probability of a significant change in expression in the peroxide-conditioned cell lines in comparison to the control group are given in electronic folder 2, available at http://www.iovs.org/cgi/content/full/43/10/3251/DC1. The genes are ranked on the basis of probability. Average signal ratios and Tukey evaluations for the first thousand genes are also presented. The probe sets are identified by Affymetrix numbers as well as by GenBank and Unigene accession numbers (GenBank and Unigene are provided in the public domain by the National Center for Biotechnology Information, Bethesda, MD, and are available at http://www.ncbi.nlm.nih.gov).

Analyses were performed on total RNA isolated from the C, H, or HT lines. For each line, four independently isolated RNA samples were used, each containing approximately 30 μg. Data from each microarray were scaled to give an overall equivalent fluorescence intensity and minimize variation. Average intensity was set at 250. For same–same comparisons, the array with the higher scaling factor was always used as the baseline. The gene array software generates a difference call based on the fluorescence intensities of the perfect match oligos versus their mismatch partners and also minimizes high and low fluorescence intensities, using the Tukey biweight analysis, thus, correcting for fluorescence intensities above the linear range or where the signal is initially below detection. If no artifacts were introduced in the preparation of the microarray, in the hybridization, or in the scaling, then there should be no difference in expression in same–same probe set comparisons.

Figure 1 shows typical scatter graphs in which the signal intensities of all genes on two arrays are plotted against each other. In Figure 1A, a comparison between two control arrays is shown. In theory, there should be no difference in signal intensity of a given probe set in the two arrays, and all points should fall on a line delineated by a ratio of 1. Indeed, the red dots delineating the probe sets present in both arrays were clustered around the no-difference line (a ratio of 1), the clustering becoming tighter as the signal intensity increases. The yellow spots denote probe sets with which the expression was marginal or have an absent call in both arrays. These probe sets were generally in the lower-signal-intensity range. Finally, the blue spots represent probe sets for which the detection call indicated the presence of the probe in one of the two arrays. The other lines indicate the ratio of the probe set intensities. The outermost lines, both above and below the ratio = 1 line, represent a ratio of four, the next lines 3 and the innermost lines 2. Most of the red dots fall within the twofold zone.

**TABLE 1.** Microarray Analysis

| Array Comparison | Increased (I) | Decreased (D) | Total (I + D) | Σ | Σ |
|---|---|---|---|---|---|
| [A] | | | | | |
| C1/C2 | 312 | 643 | 955 | 21 | 0 |
| C4/C3 | 61 | 44 | 105 | | |
| H2/H1 | 378 | 97 | 475 | 22 | |
| H4/H3 | 85 | 66 | 151 | | |
| [B] | | | | | |
| H1/C1 | 1306 | 1513 | 2819 | 1958 | 874 |
| H2/C2 | 1723 | 1304 | 3027 | | |
| H3/C3 | 984 | 1442 | 2426 | 1858 | |
| H4/C4 | 1121 | 1497 | 2618 | | |

Results obtained from array comparisons with the corrected fluorescent array signals. Comparisons are shown for arrays prepared with cDNA from cells with the same biological background [A], either C or H cells or with different biological backgrounds [B], H cells compared with C cells. Probe sets with increase in signal ratio are indicated by I and decrease by D. The Σ columns count only probe sets that appear in the comparisons being considered.

In contrast, a typical H versus C comparison (Fig. 1B) indicated a broad scattering of the signal ratios, both above and below the ratio = 1 line. Again, most of the probe sets had changes in the ratio of signal intensity of less than 2. The results indicate that stress caused a large number of changes in gene expression. However, how many of them were real is questionable.

A major basis for error in measurement of global gene expression is technical. We addressed the technical problems by using four arrays of each cell type and using statistical analysis of the data to select valid results and validate conclusions with RT-PCR. The problem of noise has been examined in the following manner.[43] Table 1 shows the results from four independent same–same comparisons. Two from the C groups and two from the H group. In a single comparison, a large number of false positives (either increase or decrease) were found. However, if two comparisons in each group are considered (i.e., the same gene must have a false call either increased or decreased in both sets to be counted), then the number of false-positive results becomes very small: twenty-one false positives in the C group and 22 in the H group. Furthermore, if all four comparisons are considered, there are no false-positive genes in common. Thus, the selection is random and disappears with additional comparisons.

In contrast, when two biologically distinct populations of RNA were examined (the H and C preparations), there were large numbers of genes with increased or decreased fluorescent signals or positive changes. By increasing the number of comparisons, the number of probe sets with positive change decreased markedly from an average of 2722 for one comparison, to 1908 for two comparisons, to 874 for four comparisons. Thus, with comparison of four microarrays with the same background, there were no false-positive results. However, a large number of genes remained in the comparison of four microarrays from conditioned lines in comparison with four control microarrays. This exercise demonstrates that noise was not a major factor and that approximately 7% of the genes appeared to have changes in their signal intensities in comparing H and C arrays. Note that the degree of change in signal was not considered in this analysis. This approach, while answering the noise question, gives no measure of the statistical significance of the observed changes.

## Statistical Analysis

A more popular method of selecting and evaluating genes that have had changes in gene expression is to use ANOVA. In this method, the probability that a gene has had a significant change in expression can be determined. Therefore, one-way ANOVA was applied to the gene population with a stringent cutoff of one false positive per 1000 genes. All three populations (12 microarrays) were examined. Thus, a significant change between any two groups would be detected, and the analytical power is considerably increased. The average difference data for the fluorescent signal for each gene was analyzed with a standard linear one-way ANOVA. A Bonferroni correction was applied to the obtained 12,422 probabilities. Genes with corrected $P < 0.001$ were considered to have been significantly affected by the treatment. To differentiate between effects of H and HT compared with C, as well as to identify differences between H and HT, these genes were subjected to a Tukey test for the contrasts H versus C, HT versus C, and HT versus H. Statistical tests were run using the "R" statistical language (see http://www.r-project.org/). Electronic folder 2 contains the probabilities of the genes. Antioxidative defense genes were selected from the 950 genes with ANOVA $P < 0.001$.

## Real-Time RT-PCR

The statistical analysis of the expression microarray data revealed a small population of antioxidative genes with significant increase in expression in the conditioned cell lines. Confirmation of some of these data were undertaken with real-time RT-PCR.[44–46] This technique is currently the most accurate method for mRNA quantitation.[46] Total RNA was used to synthesize first-strand cDNA. One microgram of total RNA from a given sample was reverse transcribed using oligo-p$(dT)_{15}$ and avian myeloblastosis virus (AMV) reverse transcriptase (first-strand cDNA synthesis kit for RT-PCR; Roche Molecular Biochemicals, Indianapolis, IN).

Real-time quantitative PCR was then used to determine cDNA and the change in gene transcription. A fluorescein PCR detection system (LightCycler; Roche Molecular Biochemicals, Indianapolis, IN) was used for this purpose.

The reactions were performed in a volume of 20 μL of mixture containing 10 pmol of each oligonucleotide primer and 2 μL green fluorescent dye (LightCycler DNA Master SYBR Green I; Roche Molecular Biochemicals) containing *Taq* DNA polymerase, reaction buffer, dNTP mixture, and SYBR green I. To determine the amount of the mRNA in a given sample, the equivalent cDNA quantity is analyzed by real-time PCR. This analysis is based on the relationship of the number of PCR cycles necessary to obtain a fluorescent signal to the amount of cDNA. A typical set of data for a glyceraldehyde-3-phosphate dehydrogenase (GAPDH) DNA standard at a number of dilutions is shown in Figure 2A. The fluorescent signals are plotted against cycle number for samples with 10-fold serial dilutions. The solution with highest concentration of DNA is detected with the smallest number of cycles. A standard curve is then constructed by the software program by plotting the log of the concentration versus the cycle number at which the signal is detected (Fig. 2B).

Melting curves of the PCR products can also be analyzed. The PCR product is heated to 95°C, annealed at 65°C, and then slowly heated again from 65°C to 95°C at 0.1°C/sec to obtain the melting profile of the preparation. The melting point for GAPDH was found to be 87.4°C. The absence of significant additional peaks indicates that essentially only one specific product was produced (data not shown). Typical melting curves obtained for two genes, GSH-*S*-transferase alpha 2 and alcohol dehydrogenase 3 are shown in Figure 2D. Again, no secondary peaks were observed. The cycle number at which the signal was detected (Fig. 2C) was used to determine the concentration of the cDNA from the GAPDH standard curve. The housekeeping genes, GAPDH and mitochondrial ribosomal protein S24 (MRPS24), served as independent internal controls. Either the GAPDH or MRPS24 concentration was determined for each cDNA sample and used to normalize all other genes tested from the same cDNA sample. The relative multiple of change in expression was recorded as the ratio of the normalized gene concentrations.

# Results and Discussion

## Conditioned Cell Line Viability

Although it is now apparent that the immortal lens epithelial cell line αTN4-1 can be conditioned to survive an $H_2O_2$ stress

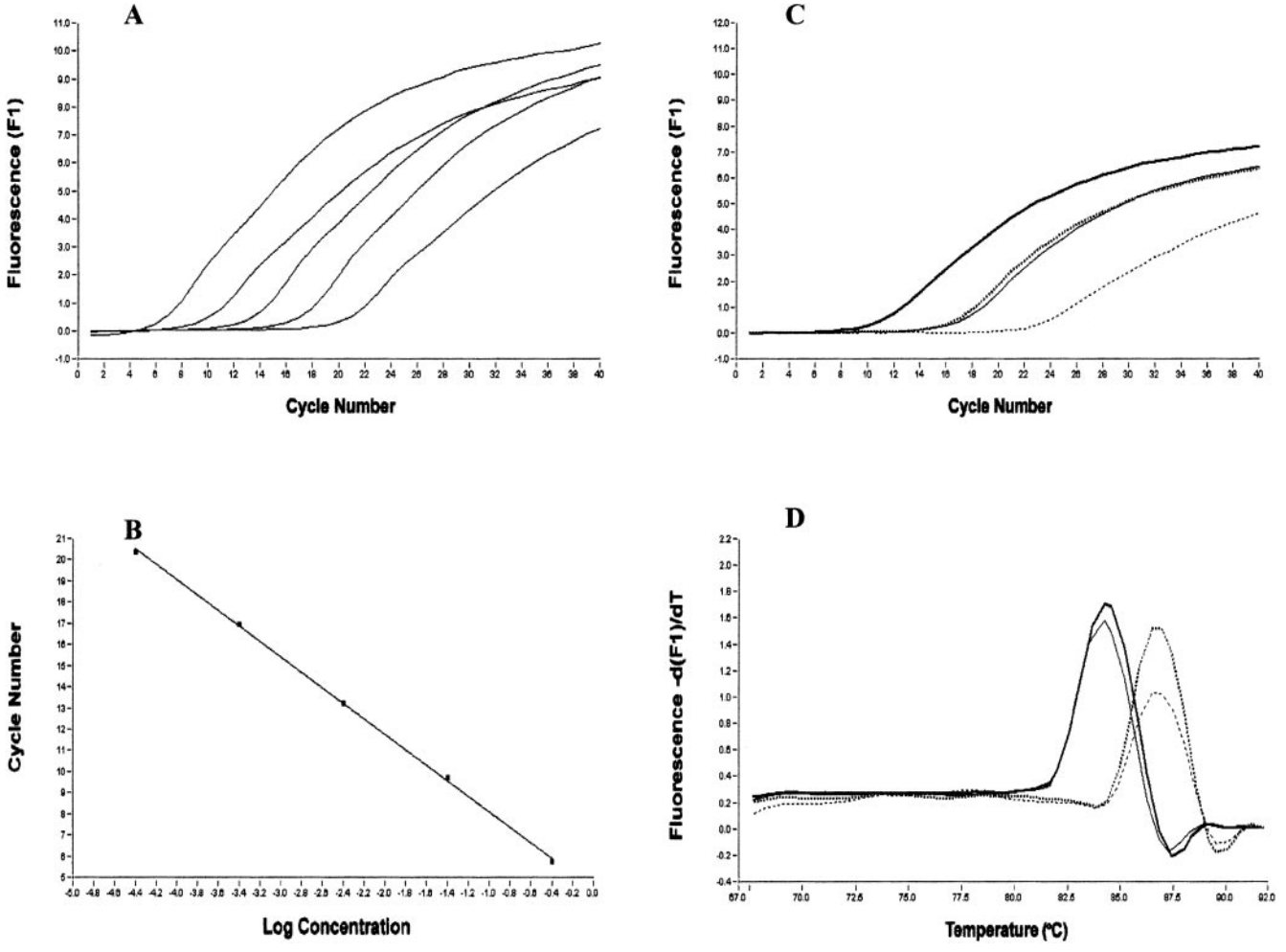


**FIGURE 2.** Real-time RT-PCR results. (**A**) Fluorescence signals of GAPDH preparations with 10-fold serial dilutions versus PCR cycle. The first solution had a concentration of $4 \times 10^{-4}$ $\mu$g and is shown on the *left*. (**B**) A standard curve for GAPDH based on results shown in (**A**). The cycle number when a fluorescent signal was detected as determined by computer extrapolation of each curve is plotted against the log of the concentration of the sample. A correlation coefficient of −1.00 was found. (**C**) Typical fluorescent signal versus PCR cycle number data for two genes GSH-*S*-transferase alpha 2 (—) and alcohol dehydrogenase 3 (– – –). The *upper curves* of each pair denote the H cell line and the *lower curves* the C cell line. (**D**) Melting curves for GSH-*S*-transferase alpha 2 (—) and alcohol dehydrogenase 3 (– – –). The *upper peaks* in each pair represent the H cell sample and the *lower peaks*, the C cell sample.

capable of killing nonconditioned cells and causing cataract in vitro,[26] these results raise certain fundamental questions, such as the ability of $H_2O_2$-conditioned cells (H), to withstand a lipid peroxide stress and how the cell biology has been altered to survive this hostile environment. As shown in Figure 3, unconditioned control (C) cells exposed to 125 $\mu$M TBHP, a lipid peroxide prototype, died only slightly slower than cells exposed to 125 $H_2O_2$ when all other conditions were the same. Cells conditioned to survive $H_2O_2$, H cells, also die when exposed to 125 $\mu$M TBHP, although at a considerably slower rate than C cells. The presence of both TBHP and $H_2O_2$ does not significantly increase the rate at which the H cells die. To gain insight into these unexpected results, H cells were exposed to gradually increasing concentrations of TBHP while continuing to add 125 $\mu$M $H_2O_2$ to the medium. After approximately 6 to 7 months, the cells were able to survive both 125 $\mu$M $H_2O_2$ and 100 $\mu$M TBHP (HT cells). These cells grew almost as rapidly as the H cells under stressing conditions. The experiments indicate that cells that have been conditioned to survive $H_2O_2$ are vulnerable to other types of peroxide stress but can be further conditioned to resist both hydrogen peroxide and lipid peroxide challenge.

## Enzyme Activities of Conditioned Cell Lines

What antioxidative defenses have been changed and enhance these cells' ability to withstand $H_2O_2$ or both $H_2O_2$ and TBHP? A number of key enzymes that degrade peroxides and superoxide were examined as well as important enzymes involved in detoxification, NADPH and adenosine triphosphate (ATP) generation and reduction of oxidized glutathione. As shown in Table 2, analysis of H cells indicated that only catalase activity was elevated markedly, increasing 136-fold. Significant but much smaller increases in activity were found with glutathione peroxidase (GSH-Px), GSH-*S*-transferase, glucose-6-phosphate dehydrogenase, and glutathione reductase (GSH red). Comparison of H cell enzyme activities over a period of a year indicated that there was some fluctuation, even though medium conditions were not altered. GSH-Px decreased 0.7-fold and catalase increased 2.2-fold. The other enzymes assayed showed little change. Thus, the overall pattern of activity was retained. It appears, however, that the H cells become increasingly dependent on catalase while minimizing GSH-Px.

In comparing enzyme activities of the HT cells with that of the H cells, little difference was found, except for GSH-*S*-

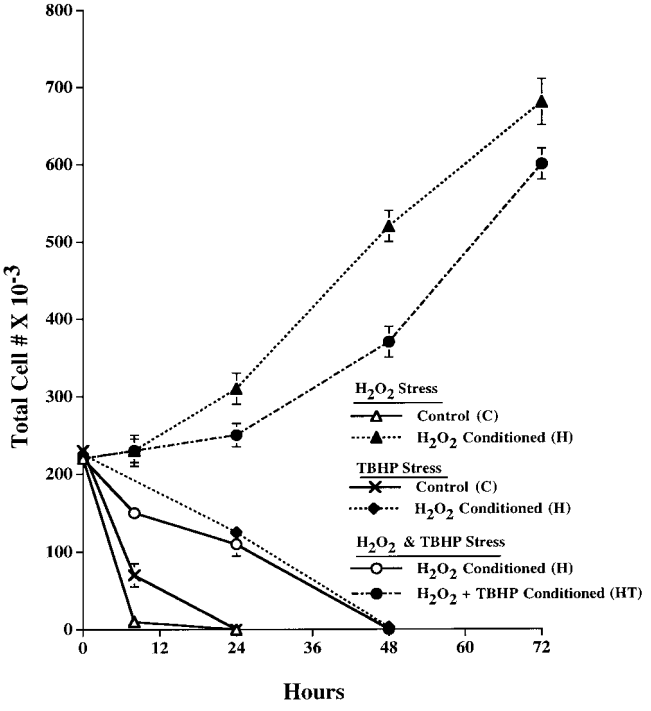


**FIGURE 3.** Cell death as a result of peroxide stress. C cells conditioned to withstand 125 $\mu$M $H_2O_2$ (H) and cells conditioned to survive 125 $\mu$M $H_2O_2$ and 100 $\mu$M TBHP (HT) were subjected to 125 $\mu$M $H_2O_2$, 125 $\mu$M TBHP, or 125 $\mu$M $H_2O_2$+100 $\mu$M TBHP. Peroxides were added every 24 hours. Cell counts were made at designated times. Results are the average of three independent experiments ± SD.

transferase, which increased 2.5-fold. It is unlikely that this change in GSH-*S*-transferase activity can completely account for the acquired resistance to TBHP.

The results obtained in comparing the enzyme activities of HT, H, and C cell preparations suggest that the few enzymes examined do not reflect the overall cellular response to oxidative stress and in the case of the HT cells, give an incomplete indication of how the cell has adjusted its biology to survive the additional oxidative stress.

## Analysis of mRNA from C and H Cells by Using Oligonucleotide Expression Arrays

To obtain information on the changes in these conditioned cell lines that may indicate how the cells survive particular oxidative stress, analysis of gene expression was initiated. For this purpose, oligonucleotide expression arrays (Affymetrix) were used. With all the cell lines, it was found that 43% to 51% of the genes and ESTs are expressed.

To detect antioxidative defense genes that have significant change in expression, a one-way ANOVA was performed on the total 12,422 genes, with the use of four C, H, and HT microarrays. The ANOVA probability for all genes is shown in electronic folder 2. The analysis is based on the actual fluorescent signals. For selection of the antioxidative defense genes, $P \leq 0.001$ was used—that is, the probability of selection of a false positive was equal or less than 1 in 1000. The genes were chosen from the list shown in electronic folder 2. In some cases in which more than one probe set for a given gene was present, it is included, even though one of the probe sets had a high ANOVA probability. Also, in some cases, a gene was selected because it either had a relatively high signal intensity in comparison to a reference group, or it was a member of a well-known antioxidative defense family. The selected 28 genes are shown in Table 3 and are ranked by probability. A brief description of the function of the gene is given as well.

The list of antioxidative defense genes contains only a few of the commonly considered members of this group. Catalase, ranked fourth, is the only enzyme usually associated with degrading $H_2O_2$. This enzyme has been shown to have a 136-fold increase in activity in H cells. Only GSH peroxidase 4, (phospholipid GSH peroxidase) of this family of peroxidases is present.

A few members of the large GSH-*S*-transferase family are listed. These enzymes detoxify products of oxidation and xenobiotics, with GSH as a cofactor. Because the different GSH-*S*-transferase classes have different specificities and cellular locations, it is not surprising to find the expression of more than one affected by peroxide stress. Whereas GSH alone can detoxify the products of reactive oxygen species (ROS), its effectiveness is directly related to its concentration. It is well established that with $H_2O_2$ stress, GSH concentrations quickly plummet in lens epithelial cell preparations and in the epithelial cell layer of the lens itself.[24,47] Thus, GSH cannot effectively protect the cell through nonenzymatic reactions for more than a very short period. However, by acting as a cofactor for the GSH-*S*-transferases, where the $K_m$ for GSH is approximately 0.1 mM,[48] 100-fold lower than the normal lens epithelial cell concentration,[49] it continues to effectively degrade the toxic products generated by $H_2O_2$. Previous work has shown that GSH-*S*-transferase alpha 1 and alpha 2 have been markedly increased at the protein level in the H cell lines.[26] Recently, it has been found that transfection of human lens epithelial cells with an alpha class GSH-*S*-transferase protects the cells against $H_2O_2$-induced lipid peroxidation.[50] It is interesting that not all detected GSH-*S*-transferase transcripts had increased expression. As shown in Table 4, the theta-1 enzyme mRNA was found to have decreased activity in both the H and HT line in relation to the C cells.

Catalase has a probability of $3.2 \times 10^{-7}$ and a 10-fold change at the mRNA level in H/C and HT/C signal intensities

**TABLE 2.** Enzyme Activities of Control and Conditioned Cells

| Enzyme | Control Cells (C) | H Cells (H) | H/C | HT Cells (HT) | HT/H |
|---|---|---|---|---|---|
| GSHPx | 24 ± 3 | 45 ± 3 | 1.9 | 48 ± 2 | 1.1 |
| Catalase | 156 ± 6 | 21,200 ± 1,200 | 136 | 20,500 ± 1,100 | 1.0 |
| Superoxide dismutase | 4,900 ± 450 | 5,300 ± 350 | 1.0 | 4,520 ± 500 | 1.0 |
| GSH-*S*-transferase* | 770 ± 72 | 1,340 ± 84 | 1.7 | 3,420 ± 87 | 2.5 |
| Glucose-6-phosphate dehydrogenase | 380 ± 24 | 742 ± 20 | 2 | 790 ± 15 | 1.1 |
| Glyceraldehyde-3-phosphate dehydrogenase | 883 ± 126 | 687 ± 93 | 0.8 | 782 | 1.1 |
| GSH reductase | 85 ± 22 | 125 ± 20 | 1.5 | 144 ± 8 | 1.2 |

* 1-chloro-2,4-dinitrobenzene was used as a substrate.

Data are expressed in milliunits per milligram protein. See Spector et al.[26] for further details concerning methodology used to determine enzyme activities.

**TABLE 3.** Antioxidative Defense Genes with Significant Change in Expression Based Primarily on ANOVA

| Rank | Gene | ANOVA *P* | Probe Set | Description |
|---|---|---|---|---|
| 1 | Hephaestin | $3.2 \times 10^{-8}$ | 104194_at | A multicopper transmembrane oxidase involved in iron transport |
| 2 | PAF acetylhydrolase | $1.2 \times 10^{-7}$ | 101923_at | PAF acetylhydrolase, same as phospholipase A2, abolishes inflammatory properties of PAF and hydrolyzes phospholipids |
| 3 | Ferredoxin 1 | $2.6 \times 10^{-7}$ | 92587_at | A powerful low-molecular-weight protein reductant |
| 4 | Catalase | $3.2 \times 10^{-7}$ | 160479_at | Catalyzed $H_2O_2$ degradation |
| 5 | Similar to NADPH-dependent leukotriene B4 12-hydroxydehydrogenase | $5.5 \times 10^{-7}$ | 98440_at | Lipid oxidoreductase deactivates leukotreine $B_3$, a potent proinflammatory factor and $\alpha$, $\beta$ unsaturated aldehydes and ketones |
| 6 | Heme oxygenase 1 | $6.1 \times 10^{-7}$ | 160101_at | Induced by oxidative stress, involved in iron metabolism and generation of antioxidants |
| 7 | Aldehyde dehydrogenase II | $1.4 \times 10^{-6}$ | 100068_at | Detoxifies toxic aldehydes generated by oxidation |
| 8 | Aldo-keto reductase 1C13 | $4.6 \times 10^{-6}$ | 95015_at | Binds NADPH and reduces a broad group of compounds |
| 9 | Reticulocalbin | $5.5 \times 10^{-6}$ | 160896_at | A calcium-binding protein located in the endoplasmic reticulum, controls calcium concentration |
| 10 | NAD(P)H menadione oxidoreductase 1 | $7.5 \times 10^{-5}$ | 94350_f_at | Catalyzes 2 electron reduction of quinones, |
| 14 | | $4.8 \times 10^{-5}$ | 94351_r_at | important antioxidative defense, $H_2O_2$ inducible |
| 11 | Epoxide hydrolase-2 | $1.6 \times 10^{-5}$ | 93051_at | Catalyze conversion of xenobiotic epoxides to diols |
| | GSH-*S*-transferase | | | |
| 12 | Microsomal | $2.1 \times 10^{-5}$ | 104742_at | GSH dependent detoxification of xenobiotics and |
| 19 | Alpha 1 | $1.5 \times 10^{-4}$ | 96085_at | products of oxidative stress |
| 24 | Alpha 3 | $1.4 \times 10^{-3}$ | 93015_at | |
| 28 | Theta 1 | $1.0 \times 10^{-2}$ | 95019_at | |
| 29 | Alpha 2 | $2.1 \times 10^{-2}$ | 101872_at | |
| 13 | Peroxiredoxin 5 | $3.5 \times 10^{-5}$ | 100332_s_at | Can reduce $H_2O_2$ and alkyl hydroperoxides |
| 15 | Alcohol dehydrogenase 3 | $5.7 \times 10^{-5}$ | 93695_at | Same as GSH-dependent formaldehyde dehydrogenase |
| 16 | Copper chaperone for superoxide dismutase 1 | $9.7 \times 10^{-5}$ | 103909_at | Delivers copper to SOD1 |
| 17 | Ferritin light chain | $1.1 \times 10^{-5}$ | 162479_f_at | An iron storage protein, regulates the free iron in the cell |
| 18 | Glutaredoxin 1 (thiol transferase) | $1.1 \times 10^{-4}$ | 95722_at | Reductant utilizes GSH as a cofactor, homologous to thioredoxin |
| 20 | Sulfide quinone reductase | $1.5 \times 10^{-4}$ | 94515_at | May detoxify sulfides |
| 21 | GSH peroxidase 4 | $1.9 \times 10^{-4}$ | 94897_at | A GSH-dependent enzyme that degrade phospholipid hydroperoxides |
| 22 | Ceruloplasmin | $7.5 \times 10^{-4}$ | 92851_at | Plasma protein involved in copper transport, scavenger of $H_2O_2$ and $O_2$, oxidizes LDL and $Fe^{+2}$, reduces $O_2$ |
| 23 | Secretory leukocyte protease inhibitor | $1.9 \times 10^{-3}$ | 92858_at | Inhibitor of serine proteases, inhibits inflammatory reactions |
| 25 | Lysosomal thiol reductase | $2.8 \times 10^{-3}$ | 97444_at | IFN-$\gamma$ inducible reductase reduces protein disulfides (related to thioredoxin) |
| 26 | Aldehyde oxidase (retinal oxidase) | $5.3 \times 10^{-3}$ | 104011_at | Converts aldehydes to acids utilizing $O_2$ as electron acceptor |
| 27 | Macrosialin (CD 68) | $6.5 \times 10^{-3}$ | 103016_s_at | Transmembrane glycoprotein, scavenges LDL |

Genes are ranked on the basis of probabilities from most to least likely to be statistically significant. Genes were primarily selected from 950 genes with $P \leq 0.001$ in a total population of 12,422 genes shown in electronic Folder 2. A few genes with greater probabilities (ranked 23–29) were also examined because of their potential antioxidative role.

and a 130-fold or more change at the activity level. It could be assumed that the combination of catalase to degrade $H_2O_2$ and the transferases to detoxify dangerous oxidized cellular components may be the only upregulated genes necessary to protect the cell, but this does not appear to be true. A variety of different classes of antioxidative defenses are present. There are some genes that regulate metal ion levels. They include hephaestin,[51] ceruloplasmin,[52–54] and ferritin[55–57] and possibly heme oxygenase.[58] Reticulocalbin[59] is also related to these genes, in that it modulates calcium concentrations. It binds calcium maintaining low cytoplasmic calcium levels that depress calcium-dependent protease activity. Hephaestin and ceruloplasmin are homologous and act in a similar manner. Ceruloplasmin oxidizes $Fe^{+2}$ to $Fe^{+3}$, facilitating iron uptake by transferrin.[51,60] It has been suggested that hephaestin also acts as a copper ferroxidase–controlling iron transport and linking copper and iron metabolism.[51] Ceruloplasmin expression is suppressed in both H and HT lines (Table 4). Ferritin, by maintaining low levels of iron and copper, minimizes Fenton-type reactions. Ferritin is the cell's major iron storage protein and regulates intracellular iron levels.[55–57] It contains both heavy and light chains with various ratios in different tissues. Mutations in the light chain gene in the iron-responsive region cause a hyperferritinemia cataract.[61–63]

Heme oxygenase (HO)-1 is induced by oxidative stress, with induction increasing with diminishing concentrations of GSH.[64,65] It degrades heme and produces antioxidant bile pigments. In the degradation of heme, iron is released. It has been suggested that HO participates in a coupled reaction with ferritin, sequestering and oxidizing the released iron and thus protecting the cell from iron catalyzed oxidation.[58] The transcriptional regulation of the gene by oxidants has led to the

TABLE 4. Additional Information on Genes Shown in Table 3

**Table 4. Additional Information on Genes Shown in Table 3**

| -2.00 +2.00 C H HT 1 2 3 4 1 2 3 4 1 2 3 4 | Gene | Probe Set | Genbank | ANOVA p-value | Fold Change | | | Tukey | | | Signal | | | | | | | | | | | |
|---|---|---|---|---|---|---|---|---|---|---|---|---|---|---|---|---|---|---|---|---|---|---|
| | | | | | H/C | HT/C | HT/H | H/C | HT/C | HT/H | C1 | C2 | C3 | C4 | H1 | H2 | H3 | H4 | HT1 | HT2 | HT3 | HT4 |
| | Hephaestin | 104194_at | AF082567 | 3.2E-08 | 1.9 | 30.2 | 20.3 | | **** | **** | 14 | 2 | 3 | 5 | 16 | 1 | 2 | 9 | 83 | 104 | 100 | 97 |
| | PAF acetylhydrolase | 101923_at | U34277 | 1.2E-07 | 11.2 | 25.7 | 2.5 | **** | **** | **** | 5 | 22 | 17 | 15 | 132 | 125 | 133 | 150 | 307 | 355 | 321 | 258 |
| | Ferredoxin 1 | 92587_at | L29123 | 2.6E-07 | 3.1 | 3.0 | -1.1 | **** | **** | | 331 | 377 | 491 | 525 | 1205 | 1206 | 1191 | 1269 | 1267 | 1461 | 1582 | 1480 |
| | Catalase | 160479_at | M29394 | 3.2E-07 | 9.8 | 9.5 | -1.0 | **** | **** | | 135 | 290 | 266 | 285 | 1859 | 1968 | 1408 | 1772 | 1820 | 1819 | 1655 | 1942 |
| | Leukotriene B4 12-hydroxydehydrogenase | 98440_at | AA596710 | 5.5E-07 | 16.1 | 15.7 | 1.1 | **** | **** | | 326 | 286 | 600 | 616 | 5541 | 5263 | 5148 | 4631 | 6032 | 4275 | 6100 | 5697 |
| | Heme oxygenase 1 | 160101_at | X56824 | 6.1E-07 | -3.0 | -3.6 | -1.2 | **** | **** | | 5515 | 5017 | 4356 | 4165 | 1863 | 1372 | 1430 | 1433 | 1272 | 1301 | 1267 | 1314 |
| | Aldehyde dehydrogenase II | 100068_at | M74570 | 1.4E-06 | -20.7 | -1.2 | 17.6 | **** | | **** | 907 | 1168 | 1114 | 1113 | 47 | 57 | 35 | 27 | 720 | 785 | 853 | 1108 |
| | Aldo-Keto reductase 1C13 | 95015_at | AB027125 | 4.6E-06 | 23.7 | 25.9 | 1.3 | **** | **** | | 45 | 16 | 65 | 95 | 1156 | 1151 | 1631 | 1570 | 1503 | 1201 | 1536 | 1747 |
| | Reticulocalbin | 160896_at | D13003 | 5.5E-06 | 3.4 | 3.0 | -1.1 | **** | **** | | 979 | 938 | 571 | 548 | 2599 | 2749 | 2444 | 2831 | 2756 | 2789 | 2080 | 2239 |
| | NAD(P)H menadione oxidoreductase 1 | 94350_f_at | U12961 | 7.5E-06 | 2.8 | 4.5 | 1.6 | **** | **** | **** | 150 | 175 | 354 | 421 | 535 | 605 | 672 | 705 | 968 | 1029 | 913 | 1000 |
| | | 94351_r_at | U12961 | 4.8E-05 | 3.0 | 3.9 | 1.4 | **** | **** | | 124 | 239 | 726 | 713 | 979 | 1197 | 1286 | 1469 | 1715 | 1912 | 1743 | 2016 |
| | Epoxide hydrolase-2 | 93051_at | Z37107 | 1.6E-05 | 6.3 | 6.4 | 1.2 | **** | **** | | 6 | 8 | 13 | 6 | 46 | 67 | 61 | 46 | 72 | 87 | 57 | 70 |
| | GSH-S-transferase, microsomal | 104742_at | AA919832 | 2.1E-05 | 8.5 | 9.5 | 1.0 | **** | **** | | 38 | 57 | 35 | 34 | 450 | 605 | 464 | 672 | 469 | 684 | 505 | 474 |
| | alpha 1 | 96085_at | L06047 | 1.5E-04 | 7.0 | 4.5 | -1.3 | **** | **** | | 262 | 348 | 1160 | 1198 | 2464 | 2361 | 2129 | 2294 | 2454 | 2078 | 2970 | 2753 |
| | alpha 3 | 93015_at | X65021 | 1.4E-03 | 3.0 | 10.8 | 6.5 | | **** | **** | 11 | 3 | 21 | 13 | 3 | 11 | 31 | 39 | 103 | 44 | 135 | 124 |
| | theta 1 | 95019_at | X98055 | 1.0E-02 | -2.7 | -1.2 | 2.3 | **** | | | 216 | 215 | 421 | 459 | 134 | 121 | 92 | 81 | 304 | 301 | 242 | 219 |
| | alpha 2 | 101872_at | J03958 | 2.1E-02 | 2.5 | 2.8 | 1.1 | | | | 1419 | 1563 | 4827 | 4580 | 5988 | 5740 | 5855 | 4370 | 6346 | 4785 | 7030 | 6255 |
| | Peroxiredoxin 5 | 100332_s_at | AF093853 | 3.5E-05 | 2.5 | 2.3 | -1.1 | **** | **** | | 977 | 896 | 1294 | 1371 | 2747 | 2886 | 2349 | 2415 | 2136 | 2154 | 2664 | 2248 |
| | Alcohol dehydrogenase 3 | 93695_at | U20257 | 5.7E-05 | 7.8 | 19.8 | 2.7 | | **** | **** | 201 | 142 | 283 | 288 | 1303 | 1421 | 1758 | 1855 | 3075 | 3060 | 5025 | 4878 |
| | Copper chaperone for superoxide dismutase1 | 103909_at | AI839702 | 9.7E-05 | 2.6 | 2.2 | -1.2 | **** | **** | | 315 | 241 | 224 | 244 | 643 | 766 | 562 | 532 | 571 | 560 | 480 | 507 |
| | Ferritin light chain | 162479_f_at | AV097950 | 1.1E-04 | 1.5 | 1.3 | -1.1 | **** | **** | | 716 | 801 | 704 | 703 | 1081 | 1214 | 1105 | 1109 | 1102 | 984 | 860 | 932 |
| | Glutaredoxin 1 (thiol transferase) | 95722_at | AB013137 | 1.1E-04 | 1.8 | 2.1 | 1.2 | **** | **** | | 118 | 84 | 119 | 118 | 176 | 232 | 159 | 173 | 288 | 237 | 238 | 234 |
| | Sulfide quinone reductase | 94515_at | AW208628 | 1.5E-04 | 1.4 | 1.6 | 1.2 | **** | **** | | 272 | 268 | 328 | 310 | 386 | 350 | 411 | 424 | 414 | 483 | 464 | 445 |
| | GSH peroxidase 4 | 94897_at | D87896 | 1.9E-04 | 1.4 | 1.2 | -1.2 | **** | | **** | 796 | 881 | 819 | 807 | 1268 | 1525 | 1175 | 1206 | 919 | 969 | 856 | 904 |
| | Ceruloplasmin | 92851_at | U49430 | 7.5E-04 | -21.6 | -23.6 | -1.9 | **** | **** | | 187 | 360 | 571 | 603 | 27 | 34 | 26 | 5 | 11 | 9 | 27 | 9 |
| | Secretory leukocyte protease inhibitor | 92858_at | AF002719 | 1.9E-03 | 121.6 | 32.6 | -4.6 | **** | | | 40 | 9 | 3 | 6 | 1078 | 824 | 1883 | 2254 | 220 | 218 | 689 | 666 |
| | Lysosomal thiol reductase | 97444_at | AI844520 | 2.8E-03 | 4.4 | 3.5 | -1.1 | **** | **** | | 50 | 79 | 76 | 67 | 351 | 371 | 220 | 211 | 220 | 460 | 271 | 302 |
| | Aldehyde oxidase (retinal oxidase) | 104011_at | AB017482 | 5.3E-03 | 4.7 | 7.2 | 2.0 | | **** | | 22 | 10 | 63 | 63 | 73 | 106 | 92 | 84 | 105 | 152 | 264 | 164 |
| | Macrosialin (CD 68) | 103016_s_at | X68273 | 6.5E-03 | 9.3 | 6.6 | -1.4 | **** | | | 47 | 13 | 40 | 50 | 550 | 310 | 209 | 218 | 273 | 262 | 187 | 205 |

Fold change and *P* values based on comparative analysis of eight arrays, determined with Affymetrix software program. Tukey analysis with a probability cutoff of 0.01 is also given.

**** Indicates a significant difference. Color bars showing the intensity of the fluorescent signals for each probe set on each array are presented, with the lowest signal indicated by the darkest color.

viewpoint that HO provides a cellular defense mechanism to oxidative stress. HO has been shown to be induced in the retina with oxidative stress and is localized exclusively in the Müller cells.[66] However, HO was suppressed in the H and HT lines.

Platelet-activating factor (PAF)-acetylhydrolases are members of a structurally distinct family of enzymes related to the phospholipases and specifically hydrolyze phospholipids, including oxidatively damaged components with a short chain at the sn-2 position. The hydrolases may detoxify oxidized phospholipid in conjunction with superoxide dismutase and GSH-Px-1.[67,68] The ferredoxins are low-molecular-weight proteins with Fe-S clusters that are ubiquitous in both animals and plants. They are powerful reductants and are involved in a broad range of reactions, including carrying electrons from ferredoxin-reductase to membrane-bound cytochrome P450, which is important in the detoxification of xenobiotics.[69,70]

NADPH-dependent leukotriene B4 12-hydroxydehydrogenase is involved in the detoxification of $\alpha,\beta$ unsaturated aldehydes and ketones. This is accomplished by the reduction of the $\alpha,\beta$ carbon-carbon double bond, using NADPH as a cofactor. The enzyme is also known as alkenal/one oxidoreductase. It is effective in reducing cytotoxic lipid peroxidation products.[71] It is striking that potent cancer chemopreventive agents upregulate a number of the genes noted on this list, including GSH-*S*-transferases, epoxide hydrolase, NADPH quinone reductase, and NADPH-dependent leukotriene B4 12-hydroxydehydrogenase.[71]

Aldehyde dehydrogenase II is a member of the large family of enzymes, including retinaldehyde dehydrogenase,[72,73] that degrade xenobiotic aldehydes.[74,75] These enzymes are involved in the metabolism of lipid peroxidation products, such as malondialdehyde and hydroxyalkenals as well as *N*-heterocyclic compounds, *N*-oxides, and nitrosamines.[73,76] Although its overall physiological function remains obscure, it is clear that it can act as an antioxidative defense component. The aldehyde dehydrogenase II gene has been recruited as a crystallin (omega-crystallin) in cephalopods.[77]

Aldo-keto reductase 1 C13 is a member of the superfamily of monomeric proteins of approximately 320 residues that metabolize a broad range of aldehydes, including xenobiotics using NAD(P)H as a cofactor. Aldose reductase, an enzyme involved in the development of sugar-induced cataract is a member of this group.[78,79] NAD(P)H menadione oxidoreductase, detoxifies quinones and quinone-imines and is capable of producing antioxidant forms of ubiquinone and vitamin E after oxidative stress.[80] It utilizes both NADH and NADPH as cofactors and uses a two-electron-reaction mechanism.[81] It has been suggested that the enzyme regulates the intracellular redox state by controlling the NAD(P)H-to-NAD(P) ratio and is induced by $H_2O_2$.[82]

Epoxide hydrolase 2 is the soluble form of the enzyme that is the major defense of the cell against xenobiotic-derived epoxides,[83–85] as well as endogenous components such as epoxides of leukotrienes.[86] The enzyme forms vicinal 1 to 2 diols that are generally less reactive than the epoxides.

Peroxiredoxins are an emerging family of antioxidant enzymes that regulate the concentrations of reactive oxygen species and protect tissues against oxidative attack.[87] Peroxiredoxin 5 is a thioredoxin peroxidase found in mitochondria, peroxisomes, and the cytosol. This peroxiredoxin is unique in forming an intramolecular disulfide intermediate that is reduced by thioredoxin.[88]

Alcohol dehydrogenase (ADH) 3 appears to be identical with formaldehyde dehydrogenase.[89] It acts on the product formed by formaldehyde and GSH, hydroxymethylglutathione. In the presence of nicotinamide adenine dinucleotide (NAD), it forms *S*-formylglutathione. It can also oxidize long-chain aliphatic alcohols and aldehydes but is not involved in retinaldehyde metabolism.[90] It, thus, contributes to the removal of toxic aldehydes possibly formed by oxidative stress.

The copper chaperone for superoxide dismutase (SOD) interacts with the Cu/Zn enzyme (SOD1) delivering copper to the enzyme. Its presence is required for SOD1 activity.[91]

Glutaredoxin, also known as thiol transferase, is a member of the thiol-disulfide oxidoreductases and has been reported as a dehydroascorbate reductase.[92,93] It appears to be important in maintaining ascorbate in its reduced form and in removing GSH and other thiols from thiolated proteins. It has been shown to protect human lens epithelial cells from $H_2O_2$ stress.[94]

Sulfide quinone reductase is an interesting protein that has been proposed to function in the detoxification and utilization of endogenous sulfides and appears to be present in eukaryotes. It is related to a mitochondrial enzyme HMT-2.[95]

GSH peroxidase (GPX) 4, the selenophospholipid hydroperoxide peroxidase (PHGPX), is an essential enzyme in protecting the cell against lethal peroxidative damage.[96,97] It differs from GPX-1 in being a monomeric protein with very different substrate specificity. GPX-4 catalyzes the direct reduction of phospholipid hydroperoxides, whereas GPX-1 is unreactive with such hydroperoxides requiring sn-1 acyl bond hydrolysis before reducing the liberated fatty acid hydroperoxide.[98,99]

Secretory leukoprotease inhibitor (SLPI) is a low-molecular-weight serine protease inhibitor[100] that also has been reported to elevate GSH levels in the lung[101] and thus may contribute directly to both antioxidative defense as well as control of deleterious protease reactions. It inhibits activation of nuclear factor (NF)-κB.[102,103]

Lysosomal thiol reductase is induced by gamma interferon, IFN-γ, and is frequently denoted as GILT. It is synthesized as a 224-amino-acid precursor that is transported to endocytic compartments. It has the ability to cleave disulfide bonds by a mechanism similar to that used by members of the thioredoxin family. It contains a CXXC motif reminiscent of the thioredoxin family of proteins. The enzyme requires a reducing agent for activation. Although L-cysteine acts in this capacity, there is no activity with glutathione.[104–106]

Aldehyde oxidase is a molybdenum dimeric enzyme that contains flavin adenine dinucleotide (FAD) and 2 Fe-S clusters and uses $O_2$ as an electron acceptor.[107,108] The enzyme has a major role in the oxidation of aldehydes, as well as the detoxification of a wide range of compounds. Recent work suggests that aldehyde oxidase is identical with retinal oxidase, converting retinaldehyde to retinoic acid.[109]

Macrosialin, a murine counterpart of human CD68, is a glycosylated transmembrane protein that scavenges low-density oxidized lipoprotein. Its overall role as an antioxidative agent is not clear at the present time.[110,111]

Additional information on these antioxidative defense genes is given in Table 4. On the left side of the table, the relative fluorescence intensity rescaled from −2 to +2 for each probe set is shown. The weaker the fluorescent signal, the darker the color. Thus, the strongest signal is denoted by white. A standard color bar is presented above the gene data. With the color depiction of the signal intensities, it is possible to assess quickly the variation in the fluorescent signal intensity of a given probe set across all 12 microarrays. The average fold change for the H/C, HT/C and HT/H comparison is given. Its reliability has been evaluated by Tukey analysis in which the probability of a real difference has been set at 0.01 or less and is indicated by asterisks. Finally, the actual corrected signal intensities are given.

Some probe sets such as hephaestin, PAF-acetylhydrolase, and epoxide hydrolase 2 have a very high probability that their gene expression has been amplified, based on both ANOVA and Tukey analysis. Yet, the signal intensities are very low, raising questions concerning their significance.

Four of these genes, aldehyde dehydrogenase II, GSH-*S*-transferase-theta, heme oxygenase 1, and ceruloplasmin have decreased expression in the conditioned cell preparations. With the latter two genes, expression is down in both the H and HT lines. Only three genes (hephaestin, GSH-*S*-transferase alpha 3, and alcohol dehydrogenase 3) clearly had amplified expression in the HT but not in the H line. With all of these genes, except alcohol dehydrogenase 3, the signal intensities are low and with the GSH-*S*-transferase, the ANOVA probability is relatively high. There are also two probe sets, macrosialin and secretory leukocyte protease inhibitor with which the expression is increased significantly, based on Tukey, only with $H_2O_2$ conditioning and one, GSH-*S*-transferase theta 1, where it is decreased. A few genes have amplified expression in the H line and a further increase in the HT line. They include PAF-acetylhydrolase, menadione oxidoreductase I, alcohol dehydrogenase 3, and possibly aldehyde oxidase. Only the first two meet the Tukey test for significance. There are some genes that are essentially not expressed in the control cell preparation but are expressed with stress. Such genes include secretory leukocyte protease inhibitor, hephaestin, and microsomal GSH-*S*-transferase.

## Real-Time RT-PCR

To obtain independent verification of the microarray data, real-time RT-PCR has been initiated with two independent internal standards: glyceraldehyde-3-phosphate dehydrogenase (GAPDH) and mitochondrial ribosomal protein S24 (MRPS24). These housekeeping genes are frequently used as internal standards because of their stability. Similar results were obtained with both internal standards. Electronic folder 3 (available at http://www.iovs.org/cgi/content/full/43/10/3251/DC1) contains the forward and reverse primers used for the real-time RT-PCR analyses. The size of the PCR products are also given. They varied from approximately 250 to 383 base pairs, with one exception of 221 base pairs. Table 5 presents Tukey, microarray, and RT-PCR data for most of the selected antioxidative defense genes. The real-time RT-PCR results, in most cases, confirm the microarray data and the Tukey evaluation. However, the actual values can be significantly different. For example, with PAF-acetylhydrolase, the microarray gave an H/C value of 11, but the RT-PCR result was 5.6 (Table 5). Both values indicate a considerable amplification in gene expression. Indeed, the point of the exercise is to select genes that have their expression significantly modified. The RT-PCR results verify that this has occurred with PAF-acetylhydrolase and this conclusion is confirmed by the Tukey analysis.

The correlation of microarray fold change with the RT-PCR results is shown in Figure 4 in which the log of the change multiples are plotted. In all cases, the trends are consistent, although with five genes, it is not possible to predict the correlation, because the change is too small to evaluate with one of the methods. If one method indicates positive or negative amplification, so does the other. However, as indicated earlier, the magnitude of the amplification is in doubt. If both methods indicated the same change multiple, the data would

**TABLE 5.** Validation of Microarray Results with Real-Time RT-PCR

| Gene | H/C Fold Change | | | | HT/C Fold Change | | | |
|---|---|---|---|---|---|---|---|---|
| | Tukey | Microarray | RT-PCR | Validation | Tukey | Microarray | RT-PCR | Validation |
| Hephaestin | — | 1.9 | X | √ | **** | 30 | X | √ |
| PAF acetylhydrolase | **** | 11 | 5.6 | √ | **** | 26 | 12 | √ |
| Ferredoxin 1 | **** | 3.1 | 2.6 | √ | **** | 3.0 | 2.4 | √ |
| Catalase | **** | 10 | 17 | √ | **** | 9.5 | 13 | √ |
| Leukotriene B4 12-hydroxydehydrogenase | **** | 16 | 42 | √ | **** | 16 | 19 | √ |
| Aldehyde dehydrogenase II | **** | −20 | Z | — | — | −1.2 | −1.3 | √ |
| NAD(P)H menadione oxidoreductase 1 | **** | 2.9 | 1.7 | √ | **** | 4.2 | 5.1 | √ |
| Epoxide hydrolase 2 | **** | 6.3 | Z | — | **** | 6.4 | Z | — |
| GSH-*S*-transferase | | | | | | | | |
| Microsomal | **** | 8.5 | 29 | √ | **** | 9.5 | 20 | √ |
| Alpha 1 | **** | 7.0 | 11 | √ | **** | 4.5 | 4.5 | √ |
| Alpha 3 | — | 3.0 | 1.0 | — | **** | 11 | 20 | √ |
| Alpha 2 | — | 2.5 | 25 | √ | — | 2.8 | 21 | √ |
| Theta 1 | **** | −2.7 | −8.0 | √ | — | −1.2 | −3.0 | √ |
| Peroxiredoxin 5 | **** | 2.5 | 3.0 | √ | **** | 2.3 | 2.9 | √ |
| Alcohol dehydrogenase 3 | — | 7.8 | 42 | √ | **** | 20 | 24 | √ |
| Copper chaperone for superoxide dismutase 1 | **** | 2.6 | 2.8 | √ | **** | 2.2 | 1.8 | √ |
| Ferritin light chain | **** | 1.5 | 1.3 | √ | **** | 1.3 | 1.6 | √ |
| Lysosomal thiol reductase | **** | 4.4 | 3.8 | √ | **** | 3.5 | 1.7 | √ |
| Aldehyde oxidase (retinal oxidase) | — | 4.7 | 1.0 | — | **** | 7.2 | 1.4 | √ |
| Macrosialin (CD 68) | **** | 9.3 | 5.2 | √ | — | 6.6 | 2.2 | √ |

The antioxidative defense genes shown in Table 3 were analyzed by Tukey statistical analysis to determine significant differences between H and C, HT and C and HT and H microarray probe set fluorescent signals. A probability cutoff of 0.01 was used. ****Indicates a significant difference. Microarray data are the average obtained from four arrays for each cell type, and RT-PCR values are the average of, in most cases, three determinations. Validation (√) indicates that the RT-PCR results validated that there was a significant change in the genes mRNA level, although the magnitude remains somewhat in doubt. In most cases, this conclusion was confirmed by the Tukey analysis of the microarray data. X indicates that RT-PCR values could be obtained for the H or HT lines but not the controls; thus, there was an increase in gene expression. Z indicates that no product could be detected by RT-PCR in either the conditioned or control preparations.

fall on the line, indicating a correlation of 1. The points are scattered around this line. In H/C comparisons for GSH-*S*-transferase alpha 3 and aldehyde oxidase, one method indicates little change in amplification, whereas the other shows definitive change. In these cases, the interpretation of whether amplification of expression occurred is in doubt. Those genes that appear to have their microarray results verified are indicated by a checkmark in the verification column.

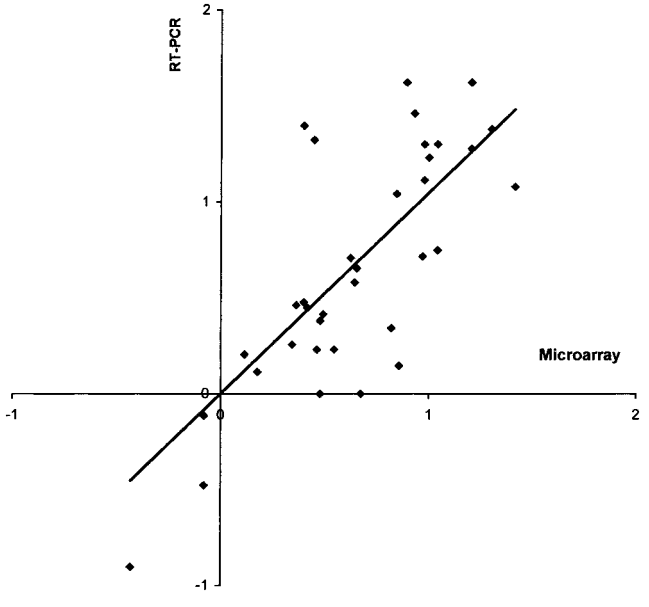


**FIGURE 4.** Correlation of RT-PCR and microarray results. The log of the fold change determined by the two procedures is given. The linear regression line is derived by $y = 1.0481x$, with a correlation coefficient of 0.77.

Another type of problem is illustrated by hephaestin. With this gene, no signal was obtain in C samples analyzed with RT-PCR and very weak signals with microarray analysis (see Table 4). Even increasing the sample amount fourfold did not produce a PCR product. However, with both H and HT cells, reasonable RT-PCR signals were obtained. Thus, gene expression was turned on, but the extent of the increased expression cannot be determined. This situation is denoted by an X in the RT-PCR column of Table 5. If no signal was obtained in any cell line (epoxide hydrolase 2) or in the H line (aldehyde dehydrogenase II), it is denoted by (Z). In the latter case, the $H_2O_2$ stress caused a marked decrease in gene expression but, again, could not be evaluated. The microarray results differ considerably from the RT-PCR values with epoxide hydrolase 2 but agree with the aldehyde dehydrogenase II and hephaestin data in a qualitative manner. Based on the these comments, verification of amplified expression was found in 35 of the 40 samples examined. Finally, in a few cases, both RT-PCR results and Tukey analysis question the microarray change multiples.

Carper et al.,[38] used differential display to examine the H and C cell lines. Increased expression was observed in a number of genes reported in their study. Of the genes they investigated, catalase had the greatest increase in expression, up 14-fold, reticulocalbin up 6-fold, and GSH-peroxidase and ferritin (both chains) up 2-fold. Metallothionein 2 was essentially unchanged. These results are in reasonable agreement with the present work, with the exception of the ferritin heavy chain, which appeared unchanged and GSH peroxidases, which may have a slight increase in gene expression.

## Expression of Classic Antioxidative Defense Genes

The surprising absence of many of the common antioxidative defenses among the genes with amplified expression led us to survey some of the members of this group (Table 6). It was

**TABLE 6.** Recognized Antioxidative Defense Genes

| Gene | Probe sets | ANOVA *P* | Fold Change | | | Signal | | | | | | | | | | | | Detection Call | | | | | | | | | | | |
|---|---|---|---|---|---|---|---|---|---|---|---|---|---|---|---|---|---|---|---|---|---|---|---|---|---|---|---|---|---|
| | | | H/C | HT/C | HT/H | C1 | C2 | C3 | C4 | H1 | H2 | H3 | H4 | HT1 | HT2 | HT3 | HT4 | C1 | C2 | C3 | C4 | H1 | H2 | H3 | H4 | HT1 | HT2 | HT3 | HT4 |
| GSH-Px 1 | 94132_at | 0.112 | 1.4 | 1.4 | −1.0 | 262 | 246 | 174 | 203 | 288 | 256 | 372 | 300 | 355 | 218 | 290 | 244 | P | P | P | P | P | P | P | P | P | P | P | P |
| GSH-Px 2 | 99810_at | 0.211 | 1.3 | 1.3 | −1.1 | 87 | 73 | 39 | 55 | 84 | 74 | 112 | 79 | 90 | 66 | 63 | 86 | P | P | P | P | P | P | P | P | P | P | M | P |
| GSH-Px 3 | 104256_at | 0.098 | 1.9 | 1.2 | −2.3 | 14 | 8 | 10 | 9 | 13 | 28 | 25 | 31 | 31 | 14 | 5 | 19 | A | A | A | A | A | A | A | A | A | A | A | A |
| GSH-Px 5 | 94692_at | 0.734 | 1.2 | 1.3 | 1.1 | 42 | 27 | 23 | 13 | 19 | 44 | 73 | 12 | 57 | 22 | 29 | 27 | A | A | A | A | A | A | A | A | A | A | A | A |
| Glutathione synthetase | 101425_at | 0.055 | 1.9 | 1.9 | 1.1 | 386 | 305 | 549 | 605 | 736 | 754 | 932 | 901 | 611 | 654 | 1074 | 1471 | P | A | P | P | P | P | P | P | M | P | P | P |
| Thioredoxin | 92807_at | 0.802 | 1.0 | −1.0 | −1.0 | 4434 | 6859 | 4259 | 4010 | 4936 | 5267 | 4921 | 5546 | 4820 | 4308 | 5208 | 4846 | P | P | P | P | P | P | P | P | P | P | P | P |
| Thioredoxin | 98130_at | 0.088 | 1.1 | −1.2 | −1.3 | 1110 | 947 | 1017 | 1111 | 1037 | 915 | 1373 | 1314 | 839 | 750 | 1022 | 947 | P | P | P | P | P | P | P | P | P | P | P | P |
| Thioredoxin reductase1 | 99985_at | 0.547 | 1.1 | 1.0 | −1.1 | 3397 | 3298 | 3939 | 4046 | 3195 | 3950 | 4790 | 4677 | 2963 | 3324 | 4368 | 4395 | P | P | P | P | P | P | P | P | P | P | P | P |
| Thioredoxin reductase1 | 161284_r_at | 0.739 | 1.1 | 1.3 | 1.0 | 574 | 293 | 409 | 585 | 369 | 422 | 629 | 400 | 552 | 338 | 565 | 631 | P | P | P | P | M | P | M | P | P | P | M | P |
| Thioredoxin reductase2 | 160437_at | 0.039 | 2.7 | 1.7 | −1.6 | 61 | 49 | 101 | 71 | 314 | 208 | 119 | 124 | 107 | 134 | 145 | 94 | P | P | P | P | P | P | P | P | P | P | P | P |
| Thioredoxin-related protein | 160115_at | 0.156 | −1.0 | −1.4 | −1.3 | 353 | 430 | 163 | 227 | 338 | 307 | 360 | 332 | 251 | 227 | 191 | 234 | P | P | P | P | P | P | P | P | A | P | P | P |
| Thioredoxin dependent peroxide reductase | 99608_at | 0.033 | −1.5 | −2.6 | −1.6 | 90 | 73 | 73 | 70 | 30 | 50 | 45 | 73 | 13 | 48 | 64 | 23 | A | P | P | P | A | A | A | A | A | A | P | A |
| Peroxiredoxins-PrxI | 97758_at | 0.452 | 1.1 | 1.2 | 1.1 | 4172 | 4407 | 4189 | 3213 | 5686 | 4076 | 3882 | 3379 | 6009 | 3250 | 6118 | 4333 | P | P | P | P | P | P | P | P | P | P | P | P |
| Peroxiredoxins-PrxII-2 | 100331_g_at | 0.169 | −1.2 | −1.3 | −1.1 | 3889 | 4077 | 2582 | 2415 | 2972 | 3280 | 2926 | 3330 | 2973 | 2753 | 1879 | 2125 | P | P | P | P | P | P | P | P | P | P | P | P |
| Peroxiredoxins-PrxII-3 | 101804_at | 0.697 | −1.2 | −1.3 | −1.0 | 11 | 5 | 18 | 6 | 9 | 7 | 10 | 5 | 9 | 7 | 9 | 9 | A | A | A | A | A | A | A | A | A | A | A | A |
| Ferritin H | 94794_at | 0.622 | −1.0 | 1.0 | 1.1 | 6127 | 7727 | 5592 | 5103 | 5570 | 5594 | 6075 | 5496 | 5831 | 4981 | 7114 | 7400 | P | P | P | P | P | P | P | P | P | P | P | P |
| Ferritin H | 161913_r_at | 0.767 | 1.2 | 1.2 | −1.1 | 3114 | 3529 | 1467 | 1665 | 3465 | 2667 | 2582 | 2588 | 3467 | 2241 | 2104 | 2436 | P | P | M | P | P | P | P | P | P | P | P | P |
| Metallothionein 1 | 93573_at | 0.337 | −1.1 | 1.1 | 1.2 | 3329 | 3276 | 3363 | 3089 | 4493 | 4482 | 2733 | 3018 | 5222 | 3515 | 3771 | 3689 | P | P | P | P | P | P | P | P | P | P | P | P |
| Metallothionein 2 | 101561_at | 0.807 | 1.2 | 1.3 | 1.1 | 3793 | 4322 | 3749 | 3410 | 5243 | 4102 | 3736 | 3514 | 5782 | 2927 | 3896 | 4082 | P | P | P | P | P | P | P | P | P | P | P | P |
| Metallothionein 3 | 95340_at | 0.421 | −1.0 | 1.2 | 1.2 | 323 | 170 | 468 | 358 | 259 | 279 | 307 | 289 | 482 | 275 | 330 | 392 | A | A | A | A | A | A | A | A | A | A | A | A |
| Metallothionein 4 | 102989_at | 0.571 | −1.4 | −1.7 | −1.3 | 14 | 41 | 6 | 6 | 13 | 11 | 13 | 11 | 14 | 6 | 13 | 5 | A | A | A | A | A | A | A | A | A | A | A | A |
| IRP-1 (aconitase 1) | 100147_at | 0.172 | −2.6 | −2.2 | 1.4 | 62 | 37 | 32 | 37 | 7 | 32 | 19 | 37 | 29 | 41 | 11 | 26 | A | A | A | A | A | A | A | A | A | A | A | A |
| Transferrin receptor | 103957_at | 0.090 | −1.8 | −1.2 | 1.5 | 248 | 209 | 205 | 133 | 93 | 85 | 107 | 160 | 243 | 205 | 126 | 108 | P | P | P | P | P | P | P | P | P | P | P | P |
| Transferrin receptor | 103958_g_at | 0.113 | −1.3 | −1.0 | 1.3 | 1753 | 1292 | 1477 | 1214 | 1112 | 889 | 1397 | 1276 | 1844 | 1278 | 1446 | 1643 | P | P | P | P | P | P | P | P | P | P | P | P |
| Phospholipase A2-V | 101328_at | 0.170 | −1.4 | 1.2 | 1.4 | 85 | 52 | 167 | 146 | 51 | 61 | 60 | 78 | 87 | 69 | 140 | 141 | P | A | P | P | A | P | A | P | P | P | P | P |
| Phospholipase A2-V | 94665_at | 0.682 | −1.2 | −1.2 | 1.1 | 79 | 53 | 168 | 137 | 72 | 64 | 116 | 90 | 83 | 51 | 173 | 143 | A | A | P | P | A | A | A | M | A | A | P | P |
| Phospholipase A2-IIA | 92735_at | 0.476 | 1.5 | 1.3 | −1.2 | 11 | 15 | 12 | 9 | 12 | 13 | 25 | 16 | 13 | 22 | 11 | 10 | A | A | A | A | A | A | A | A | A | A | A | A |
| Phospholipase A2-Ca-independent | 97965_at | 0.149 | −2.3 | −2.7 | −1.8 | 113 | 69 | 155 | 160 | 30 | 83 | 132 | 148 | 72 | 55 | 88 | 23 | A | A | P | P | A | A | A | M | A | A | A | A |
| Phospholipase A2-IIC | 99326_at | 0.064 | 2.0 | 1.6 | −1.3 | 105 | 65 | 53 | 51 | 111 | 136 | 108 | 120 | 150 | 69 | 86 | 90 | A | A | A | A | A | P | A | A | A | A | A | A |
| NADPH-cytochrome P450 reductase | 99019_at | 0.461 | 1.1 | −1.1 | −1.2 | 544 | 420 | 706 | 678 | 481 | 491 | 674 | 547 | 503 | 520 | 520 | 464 | P | P | P | P | P | P | P | P | P | P | P | P |

A group of genes frequently associated with antioxidative defenses is shown. Probe set numbers are given as well as probabilities and fold change. The fluorescent signal values for each of the C, H, and HT arrays and the detection call based on the microarray software analysis are also presented.

found that none of the GSH peroxidases except phospholipid GSH peroxidase was significantly amplified (ANOVA, $P = 0.1$–0.7) lending further support to the viewpoint that GSH-Pxs have limited roles as antioxidant defense enzymes and that the absence of GSH-Px-1 does not compromise animal viability.[112] The thioredoxins and peroxiredoxins (except for peroxiredoxin 5) also showed little change. Nor was there a significant amplified expression of the phospholipase A2 family, which is believed to be involved in degradation of membrane lipid peroxides. Although the ferritin light chain appeared to have an increased expression, two different probe sets for the heavy chain showed no significant change in expression. On the basis of the present data, it appears that many of the well-defined antioxidative genes do not have amplified expression in the conditioned lens epithelial cell lines.

Many of the genes and ESTs which have amplified expression in the conditioned cells do not appear to be involved in antioxidative defense systems. There are a number of possible explanations for this situation. Some of these genes may be clustered on exposed segments of chromosomes in the vicinity of key antioxidative genes that have amplified expression and thus also have increased transcription. These genes may have promoters, enhancers, or other control elements, including oxidation-responsive elements in common, leading to their increased expression. It is also possible that the amplified expression of the antioxidative defense genes causes the cell to readjust its overall biology, leading to the observed expression pattern. It also appears that the cell reorganizes its overall structure, shifting gene expression to respond more effectively to its altered environment.[113] Further analysis of these genes is in progress to gain insight into their relationship with antioxidative defenses.

Based on this work, a relatively small number of antioxidative genes have their expression significantly amplified in response to peroxide stress and an even smaller number are found when already conditioned H cells are subjected to a different peroxide, TBHP. (It is possible that the presence of both $H_2O_2$ and TBHP obscures the cell's response to just one stressing agent. Therefore, a cell line conditioned to resist only TBHP has been developed and is now being analyzed.) This suggests that there are a few key antioxidative components that determine whether a cell will survive a particular stress and that the same genes may not be involved or may not be sufficient to respond to other closely allied stresses. Some of the identified genes have not been previously considered in examination of the lens' antioxidative defenses. Although, in most cases, the results obtained by microarray expression analysis have been verified by real-time RT-PCR, further work is needed at the protein level to confirm the conclusions drawn from this study.

The analysis presented in this article considers approximately 12,400 genes and ESTs. Although there is no certainty about the total number of genes in the mouse genome, it is probable, based on the human genome work, that there are only approximately 30,000 genes in the genome.[114–116] On this basis, our work has examined approximately one third of the mouse genome. It will be interesting to find whether other important antioxidative systems will be revealed when the remainder of the genome is examined and annotation of genes with unknown function is completed.

## *Acknowledgments*

The authors thank Vladan Miljkovic, Manager of the Gene MicroArray Facility of Columbia University, for his assistance with the expression microarray hybridization and initial analysis.

## *References*

1. Bray TM. Antioxidants and oxidative stress in health and disease: introduction. *Proc Soc Exp Biol Med.* 1999;222:195.
2. Forsberg L, deFaire U, Morgenstern R. Oxidative stress, human genetic variation and disease. *Arch Biochem Biophys.* 2001;389:84–93.
3. Hoeschen RJ. Oxidative stress and cardiovascular disease. *Can J Cardiol.* 1997;13:1021–1025.
4. Singal PK, Khaper N, Palace V, Kumar D. The role of oxidative stress in the genesis of heart disease. *Cardiovasc Res.* 1998;40:426–432.
5. Thomson A, Hemphilly D, Jeejeebhog KN. Oxidative stress and antioxidants in intestinal disease. *Dig Disease.* 1998;16:152–158.
6. Koyama H, Geddes DM. Genes, oxidative stress and the risk of chronic obstructive pulmonary disease. *Thorax.* 1998;53(suppl 2):S10–S14.
7. Esposito LA, Melov S, Panov A, Cottrell BA, Wallace DC. Mitochondrial disease in the mouse results in increased oxidative stress. *Proc Natl Acad Sci USA.* 1995;96:4820–4825.
8. Sayre LM, Smith MA, Perry G. Chemistry and biochemistry of oxidative stress in neurodegenerative disease. *Curr Med Chem.* 2001;8:721–738.
9. Smith MA, Rottkamp CH, Nunomura A, Raina AK, Perry G. Oxidative stress in Alzheimer's disease. *Biochim Biophys Acta.* 2000;1502:139–144.
10. Cohen G. Oxidative stress, mitochondrial respiration and Parkinson's disease. *Ann NY Acad Sci.* 2000;899:112–120.
11. Spector A. The search for a solution to senile cataracts: Proctor Lecture. *Invest Ophthalmol Vis Sci.* 1984;25:130–146.
12. Varma SD, Chand D, Sharma YR, Kuck JF Jr, Richards RD. Oxidative stress on lens and cataract formation: role of light and oxygen. *Curr Eye Res.* 1984;3:35–38.
13. Babizhaev MA, Deev AI. Free radical oxidation of lipids and thiol groups in formation of a cataract. *Biofizika.* 1986;31:109–114.
14. Spector A. The lens and oxidative stress. In: Sies H, ed. *Oxidative Stress, Oxidants and Antioxidants.* London: Academic Press; 1991:529–558.
15. Zigman S, Paxhia T, McDaniel T, Lou MF, Yu NT. Effect of chronic near-ultraviolet radiation on the gray squirrel lens in vivo. *Invest Ophthalmol Vis Sci.* 1991;32:1723–1732.
16. Giblin FJ, Padgaonkar VA, Leverenz VR, et al. Nuclear light scattering, disulfide formation and membrane damage in lenses of older guinea pigs treated with hyperbaric oxygen. *Exp Eye Res.* 1995;60:219–235.
17. Spector A, Wang G-M, Wang R-R, Li W-C, Kuszak JR. A brief photochemically induced oxidative insult causes irreversible lens damage and cataract. I: transparency and epithelial cell layer. *Exp Eye Res.* 1995;60:471–481.
18. Balasubramanian D. Ultraviolet radiation and cataract. *J Ocul Pharmacol Ther.* 2000;16:285–297.
19. Spector A, Garner WH. Hydrogen peroxide and human cataract. *Exp Eye Res.* 1981;33:673–681.
20. Ramachandran S, Morris SM, Devamonoharan PS, Henein M, Varma SD. Radio-isotopic determination of hydrogen peroxide in aqueous humor and urine. *Exp Eye Res.* 1991;53:503–506.
21. Bhuyan DK, Camras CB, Lakhani HK, Bhuyan KC. Peroxide concentration in normal and cataractous human lenses [ARVO Abstract]. *Invest Ophthalmol Vis Sci* 1992;33(4):**S**798. Abstract nr 531.
22. Dische Z, Zil H. Studies on the oxidation of cysteine to cystine in lens proteins during cataract formation. *Am J Ophthalmol.* 1951;34:104–113.
23. Augusteyn RC. Protein modification in cataract: possible oxidative mechanisms. In: Duncan G, ed. *Mechanisms of Cataract Formation in the Human Lens.* New York: Academic Press; 1981:72–115.
24. Spector A. Oxidative stress-induced cataract: mechanism of action. *FASEB J.* 1995;9:1173–1182.
25. Spector A, Wang G-M, Wang R-R., Li W-C, Kleiman NJ. A brief photochemically induced oxidative insult causes irreversible lens damage and cataract. II: mechanism of action. *Exp Eye Res.* 1995;60:483–493.

26. Spector A, Wang R-R, Ma W, Kleiman NJ. Development and characterization of a $H_2O_2$ resistant immortal lens epithelial cell line. *Invest Ophthalmol Vis Sci.* 2000;41:832–843.
27. Guillen E, Abeijon C, Hirschberg CB. Mammalian Golgi apparatus UDP-N-acetylglucosamine transporter: molecular cloning by phenotypic correction of a yeast mutant. *Proc Natl Acad Sci USA.* 1998;95:7888–7892.
28. Matern HT, Yeaman C, Nelson WJ, Scheller RH. The Sec6/8 complex in mammalian cells: characterization of mammalian Sec3, subunit interactions, and expression of subunits in polarized cells. *Proc Natl Acad Sci USA.* 2001;98:9648–9653,
29. Marks B, Stowell MH, Vallis Y, et al. GTPase activity of dynamin and resulting conformation change are essential for endocytosis. *Nature*. 2001;410:231–235.
30. Lanzetti L, Rybin V, Malabarba MG, et al. The Eps8 protein coordinates EGF receptor signalling through Rac and trafficking through Rab5. *Nature*. 2000;408:374–377.
31. Runnels LW, Yue L, Clapham DE. TRP-PLIK, a bifunctional protein with kinase and ion channel activities. *Science*. 2001;291: 1043–1047.
32. Molinari M, Helenius A. Chaperone selection during glycoprotein translocation into the endoplasmic reticulum. *Science*. 2000;288: 331–333.
33. Kato H, Tjernberg A, Zhang W, et al. SYT associates with human SNF/SWI complexes and the C-terminal region of its fusion partner SSX1 targets histones. *J Biol Chem.* 2002;277:5498–5505.
34. Mach CM, Hargrove BW, Kunkel GR. The small RNA gene activator protein, SphI postoctamer homology-binding factor/selenocysteine tRNA gene transcription activating factor, stimulates transcription of the human interferon regulatory factor-3 gene. *J Biol Chem.* 2002;277:4853–4858.
35. Raucher D, Stauffer T, Chen W, et al. Phosphatidylinositol 4,5-bisphosphate functions as a second messenger that regulates cytoskeleton-plasma membrane adhesion. *Cell*. 2000;100:221–228.
36. Fisk HA, Winey M. The mouse Mps1p-like kinase regulates centrosome duplication. *Cell*. 2001;106:95–104.
37. Li DW-C, Spector A. Hydrogen peroxide-induced expression of the proto-oncogenes, c-*jun*, c-*fos* and c-*myc* in rabbit lens epithelial cells. *Mol Cell Biochem*. 1997;173:59–69.
38. Carper D, John M, Chen Z, et al. Gene expression analysis of an $H_2O_2$-resistant lens epithelial cell line. *Free Rad Biol Med.* 2001; 31:90–97.
39. Carper DA, Sun JK, Iwata T, et al. Oxidative stress induces differential gene expression in a human lens epithelial cell line. *Invest Ophthalmol Vis Sci.* 1999;40:400–406.
40. Novak JP, Sladek R, Hudson TJ. Characterization of variability in large-scale gene expression data: implication for study design. *Genomics.* 2002;79:104–113.
41. Lockhart DJ, Dang H, Byrne MC, et al. Expression monitoring by hybridization to high-density oligonucleotide arrays. *Nat Biotechnol.* 1996;14:1675–1680.
42. Jacobuzio-Donahue CA, Maitra A, Shen-Ong GL, et al. Discovery of novel tumor markers of pancreatic cancer using global gene expression technology. *Am J Path.* 2002;160:1239–1249.
43. Mills JC, Gordon JI. A new approach for filtering noise from high-density oligonucleotide micro-array data sets. *Nucleic Acid Res.* 2001;29:1–13.
44. Kaiser K, Rabodonirina M, Picot S. Real time quantitative PCR and RT-PCR for analysis of pneumocystis carnihominis. *J Microbiol Methods*. 2001;45:113–118.
45. Rajeevan MS, Vernon SD, Taysavang N, Unger ER. Validation of array-based gene expression profiles by real time (kinetic) RT-PCR. *J Mol Diagn.* 2001;3:26–31.
46. Higuchi R, Fockler C, Dolinger G, Watson R. Kinetic PCR analysis-real time monitoring of DNA amplification. *Biotechnol*. 1993;11: 1026–1030.
47. Spector A, Huang R-RC, Wang G-M, Schmidt C, Yan G-Z, Chifflet S. Does elevated glutathione protect the cell from $H_2O_2$ insult? *Exp Eye Res.* 1987;45:453–465.
48. Ketterer B. Protective role of glutathione and glutathione transferases in mutagenesis and carcinogenesis. *Mutat Res*. 1988;202:343–361.
49. Reddy VN. Glutathione and its function in the lens: an overview. *Exp Eye Res.* 1990;50:771–778.
50. Yang Y, Sharma R, Cheng J. -Z, et al. Protection of HLE B-3 cells against hydrogen peroxide and naphthalene-induced lipid peroxidation and apoptosis by transfection with hGSTA1 and hGSTA2. *Invest Ophthalmol Vis Sci.* 2002;43:434–445.
51. Vulpe CD, Kuo Y-M, Murphy TL, et al. Hephaestin, a ceruloplasmin homologue implicated in intestinal iron transport, is defective in the sla mouse. *Nat Genet.* 1999;21:195–199.
52. Mzhel'skaya TI. Biological functions of ceruloplasmin and their deficiency caused by mutation in genes regulating copper and iron metabolism. *Bull Exp Biol Med*. 2000;130:719–727.
53. Rydén L. Ceruloplasmin. In: Lontie R, ed. *Copper Proteins and Copper Enzymes*. Vol 3. Boca Raton, FL: CRC Press; 1984:37–100.
54. Saenko EL, Yaropolov AI, Harris ED. Biological functions of ceruloplasmin expressed through copper-binding sites and a cellular receptor. *J Trace Elem Exp Med.* 1994;7:69–88.
55. Crichton RR, Charloteauz-Wauters M. Iron transport and storage. *Eur J Biochem.* 1987;164:485–506.
56. Aisen P. Iron transport and storage proteins. *Annu Rev Biochem.* 1980;49:357–393.
57. Harrison PM, Arosio P. Ferritins: Molecular properties, iron storage function and cellular regulation. *Biochim Biophys Acta.* 1996;1275:161–203.
58. Vile GF, Basa-Modak S, Waltner C, Tyrrell RM. Heme oxygenase 1 mediates an adaptive response to oxidative stress in human skin fibroblasts. *Proc Natl Acad Sci USA.* 1994;91:2607–2610.
59. Ozawa M, Muramatsu T. Reticulocalbin, a novel endoplasmic reticulum resident $Ca^{2+}$-binding protein with multiple EF hand motifs and a carboxyl-terminal HDEL sequence. *J Biol Chem.* 1993;268:699–705.
60. Syed BA, Beaumont NJ, Patel A, et al. Analysis of the human hephaestin gene and protein: comparative modelling of the N-terminus ecto-domain based upon ceruloplasmin. *Prot Eng*. 2002;15:205–214.
61. Cheng Q, Gonzalez P, Zigler JS Jr. High level of ferritin light chain mRNA in lens. *Biochem Biophys Res Commun*. 2000;270:349–355.
62. Beaumont C, Leneuve P, Devaux I, et al. Mutation in the iron responsive element of the L-ferritin mRNA in a family with dominant hyperferritinaemia and cataract. *Nat Genet*. 1995;11:444–445.
63. Girelli D, Corrocher R, Bisceglia L, et al. Hereditary hyperferritinemia-cataract syndrome caused by a 29-base pair deletion in the iron responsive element of ferritin L-subunit gene. *Blood*. 1997; 90:2084–2088.
64. Ryter SW, Tyrrell RM. The heme synthesis and degradation pathways: role in oxidant sensitivity. *Free Rad Biol Med*. 2000; 28:289–304.
65. Shelton KR, Egle PM, Todd JM. Evidence that glutathione participates in the induction of a stress protein. Biochem. *Biophys Res Commun*. 1986;134:492–498.
66. Ulyanova T, Agoston S, Kutty RK, et al. Oxidative stress induces heme oxygenase-1 immunoreactivity in Müller cells of mouse retina in organ culture. *Invest Ophthalmol Vis Sci.* 2001;42:1370–1374.
67. Soubeyr S, Manjunath P. Platelet-activating factor acetylhydrolase in seminal plasma: a brief review. *Mol Rep Dev*. 1998;50:510–519.
68. Parks JE, Hough SR. Platelet activating factor acetylhydrolase activity in bovine seminal plasma. *J Androl*. 1993;14:335–339.
69. Grinberg AV, Hannemann F, Schiffler B, Muller J, Heinemann U, Bernhardt R. Adrenodoxin: structure, stability and electron transfer properties. *Proteins.* 2000;40:590–612.
70. Xia B, Jenk D, LeMaster DM, Westler WM, Markley JL. Electron-nuclear interactions in two prototypical (2Fe-2S) proteins: Selective (chiral/deuteration) and analysis of $^1H$ and $^2H$ NMR signals from the alpha and beta hydrogens of cysteinyl residues that ligate the iron in the active sites of human ferredoxin and anabaena 7120 vegetative ferredoxin. *Arch Biochem Biophys.* 2000;373:328–334.
71. Dick RA, Kwak MI-K, Sutter TR, Kensler TW. Antioxidative function and substrate specificity of NAD(P)H dependent alkenal/one oxidoreductase. *J Biol Chem.* 2001;276:40803–40810.
72. Tomita S, Tsujita M, Ichikawa Y. Retinal oxidase identical to aldehyde oxidase. *FEBS Lett*. 1993;336:272–274.
73. Huang D-Y, Aizo F, Ichikawa Y. Molecular cloning of retinal oxidase/aldehyde oxidase cDNAs from rabbit and mouse livers and functional expression of recombinant mouse retinal oxidase

cDNA in Escherichia coli. *Arch Biochem Biophys.* 1999;364:264–272.
74. Cheung C, Smith CK, Hoog J-O, Hotchkiss SAM. Expression and localization of human alcohol and aldehyde dehydrogenase enzymes in skin. *Biochem Biophys Res Commun*. 1999;261:100–107.
75. Grünn F, Hirase Y, Kawauchi S, Ogura T, Umesono K. Aldehyde dehydrogenase 6, a cytosolic retinaldehyde dehydrogenase prominently expressed in sensory neuroepithelia during development. *J Biol Chem.* 2000;275:41210–41218.
76. Yoshihara S, Tatsumi K. Purification and characterization of hepatic aldehyde oxidase in male and female mice. *Arch Biochem Biophys.* 1997;338:29–34.
77. Piatigorsky J, Kozmik Z, Horwitz J, et al. Omega-crystallin of the scallop lens: a dimeric aldehyde dehydrogenase class 1/2 enzyme-crystallin. *J Biol Chem.* 2000;275:41064–41073.
78. Jez JM, Bennett MJ, Schlegel BP, Lewis M, Penning TM. Comparative anatomy of the aldo-keto reductase superfamily. *Biochem J.* 1997;326:625–636.
79. Ikeda S, Okuda-Ashitaka E, Masu Y, et al. Cloning and characterization of two novel aldo-keto reductases (AKR1C12 and ACK1C13) from mouse stomach. *FEBS Lett.* 1999;459:433–437.
80. Siegel D, Ross D. Immunodetection of NAD(P)H: quinone oxidoreductase I (NQOI) in human tissues. *Free Radic Biol Med*. 2000;29:246–253.
81. Chen S, Knox R, Wu K, et al. Molecular basis of the catalytic differences among DT-diaphorase of human, rat and mouse. *J Biol Chem.* 1997;272:1437–1439.
82. Bello RI, Diaz CG, Navarro F, Acain J, Villalba JM. Expression of NAD(P)H: quinone oxidoreductase 1 in HeLa cells. *J Biol Chem.* 2001;276:44379–44384.
83. Argiriadi MA, Morisseau C, Hammock BD, Christianson DW. Detoxification of environmental mutagens and carcinogens: structure, mechanism, and evolution of liver epoxide hydrolase. *Proc Natl Acad Sci USA.* 1999;96:10637–10642.
84. Greene JF, Newman, JW, Williamson KC, Hammock BD. Toxicity of epoxy fatty acids and related compounds to cells expressing human soluble epoxide hydrolase. *Chem Res Toxicol*. 2000;13:217–226.
85. Omiecinski CJ, Hassett C, Hosagrahara V. Epoxide hydrolase: polymorphism and role in toxicology. *Toxicol Lett.* 2000;112–113:365–370.
86. Haeggstrom JZ, Wetterholm A, Medina JF, Samuelsson B. Novel structural and functional properties of leukotriene A4 hydrolase: implications for the development of enzyme inhibitors. *Adv Prostaglandin Thomboxane Leukot Res.* 1994;22:3–12.
87. Declercq J-P, Evrard C, Clippe A, Stricht DV, Bernard A, Knoops B. Crystal structure of human peroxiredoxin 5, a novel type of mammalian peroxiredoxin at 1.5 Å resolution. *J Mol Biol.* 2001;311:751–759.
88. Seo MS, Kang SW, Kim K, Baines IC, Lee TH, Rhee SG. Identification of a new type of mammalian peroxiredoxin that forms an intramolecular disulfide as a reaction intermediate. *J Biol Chem.* 2000;275:20346–20354.
89. Koivusalo M, Baumann M, Uotila L. Evidence for the identity of glutathione-dependent formaldehyde dehydrogenase and class III alcohol dehydrogenase. *FEBS Lett.* 1989;257:105–109.
90. Duester, G. Alcohol dehydrogenase as a critical mediator of retinoic acid synthesis from vitamin A in the mouse embryo. *J Nutr.* 1998;128(suppl):4595–4625.
91. Kato S, Sumi-Akamaru H, Fujimura H, et al. Copper chaperone for superoxide dismutase co-aggregates with superoxide dismutase 1 (SOD1) in neuronal Lewy body-like hyaline inclusions: an immunohistochemical study on familial amyotrophic lateral sclerosis with SOD1 gene mutation. *Acta Neuropathol.* 2001;102:233–238.
92. Meyer EB, Wells WW. Thiol transferase overexpression increases resistance of MCF-7 cells to Adriamycin. *Free Radic Biol Med.* 1999;26:770–776.
93. Wells WW, Xu CP, Yang Y, Rocque PA. Mammalian thiol transferase (glutaredoxin) and protein disulfide isomerase have dehydroascorbate reductase activity. *J Biol Chem.* 1990;265:15361–15364.
94. Xing KY, Lou MF. Effect of $H_2O_2$ on human lens epithelial cells and the possible mechanism for oxidative damage repair by thiol transferase. *Exp Eye Res.* 2002;74:113–122.
95. Bronstein M, Schutz M, Hanska G, Padan E, Shahak Y. Cyanobacterial sulfide-quinone reductase: cloning and heterologous expression. *J Bacteriol.* 2000;182:3336–3344.
96. Hurst R, Korytowski W, Kriska T, Esworthy RS, Chu FF, Girotti AW. Hyper resistance to cholesterol hydroperoxide-induced peroxidative injury and apoptotic death in a tumor cell line that overexpresses glutathione peroxidase isotype-4. *Free Radic Biol Med*. 2001;31:1051–1065.
97. Ursini F, Maiorini M, Sevanian A. Membrane hydroperoxides. In: Sies H, ed. *Oxidative Stress: Oxidants and Antioxidants.* New York: Academic Press; 1991:319–336.
98. Grossman A, Wendel A. Non-reactivity of the selenoenzyme glutathione peroxidase with enzymatically hydroperoxidized phospholipids. *Eur J Biochem.* 1983;135:549–552.
99. Van Kuijk FJGM, Sevanian A, Handelman GJ, Dratz EA. A new role for phospholipase A2: protection of membranes from lipid peroxidation damage. *Trends Biochem Sci.* 1987;12:31–34.
100. Kikuchi T, Abe T, Yaekashiwa M, et al. Secretory leukoprotease inhibitor augments hepatocyte growth factor production in human lung fibroblasts. *Am J Respir Cell Mol Biol.* 2000;3:364–370.
101. Gillissen A, Birrer P, McElvaney NG, et al. Recombinant secretary leukoprotease inhibitor augments glutathione levels in lung epithelial lining fluid. *J Appl Physiol.* 1993;75:825–832.
102. Mulligan MS, Lentsch AB, Luber-Lang M, et al. Anti-inflammatory effects of mutant forms of secretory leukocyte protease inhibitor. *Am J Pathol.* 2000;156:1033–1039.
103. Lentsch AB, Jord JA, Czemak BJ, et al. Inhibition of NF-κB activation and augmentation of IκBβ by secretory leukocyte protease inhibitor during lung inflammation. *Am J Pathol.* 1999;154:239–247.
104. Arunachalam B, Phan UT, Geuze HJ, Cresswell P. Enzymatic reduction of disulfide bonds in lysosomes: characterization of a gamma-interferon-inducible lysosomal thiol reductase (GILT). *Proc Natl Acad Sci USA.* 2000;97:745–750.
105. Phan UT, Arunachalam B, Cresswell P. Gamma-interferon-inducible lysosomal thiol reductase (GILT). *J Biol Chem.* 2000;275:25907–25914.
106. Phan UT, Maric M, Dick TB, Cresswell P. Multiple species express thiol oxidoreductases related to GILT. *Immunogenetics.* 2001;53:342–346.
107. Rajagopalan K. Xanthine oxidase and aldehyde oxidase. In: Jakoby WB, ed. *Enzymatic Basis of Detoxification.* New York: Academic Press; 1980:294–307.
108. Al-Salmy HS. Individual variation in hepatic aldehyde oxidase activity. *Life.* 2001;51:249–253.
109. Tsuijita M, Tomita S, Miura S, Ichikawa Y. Characteristic properties of retinal oxidase (retinoic acid synthase from rabbit hepatocytes. *Biochim Biophys Acta.* 1994;1204:108–116.
110. Gough PJ, Gordon S, Greaves DR. The use of human CD68 transcriptional regulatory sequences to direct high-level expression of class A scavenger receptor in macrophages *in vitro* and *in vivo*. *Immunology.* 2001;103:351–361.
111. Rabinowitz SS, Gordon S. Macrosialin, a macrophase-restricted membrane sialoprotein differentially glycosylated in response to inflammatory stimuli. *J Exp Med.* 1991;174:827–836.
112. Spector A, Kuszak JR, Ma W, Wang R-R The effect of aging on glutathione peroxidase-1 knockout mice: resistance of the lens to oxidative stress. *Exp Eye Res.* 2001;72:533–545.
113. Oleynikov YS, Sun F, Spector A. Cell morphology and cytoskeletal disruption in lens epithelial cell lines subjected to peroxide stress. ARVO Abstract 2373, 2002.
114. Venter C, Adams MD, Myers EW, et al. The sequence of the human genome. *Science.* 2001;291:1304–1351.
115. Claverie JM. What if there are only 30,000 human genes? *Science.* 2001;291:1255–1257.
116. The International Mouse Mutagenesis Consortium. Functional annotation of mouse genome sequences. *Science*. 2001;291:1251–1255.